AD-A078 828 TEXAS UNIV AT AUSTIN DEPT OF MECHANICAL ENGINEERING F/G 11/4
INTERFACE CHARACTER OF ALUMINUM/GRAPHITE METAL MATRIX COMPOSITE--ETC(U)
DEC 79 H L MARCUS , D LASER N00014-78-C-0094

UNCLASSIFIED NL

| OF |
AD-
A078828

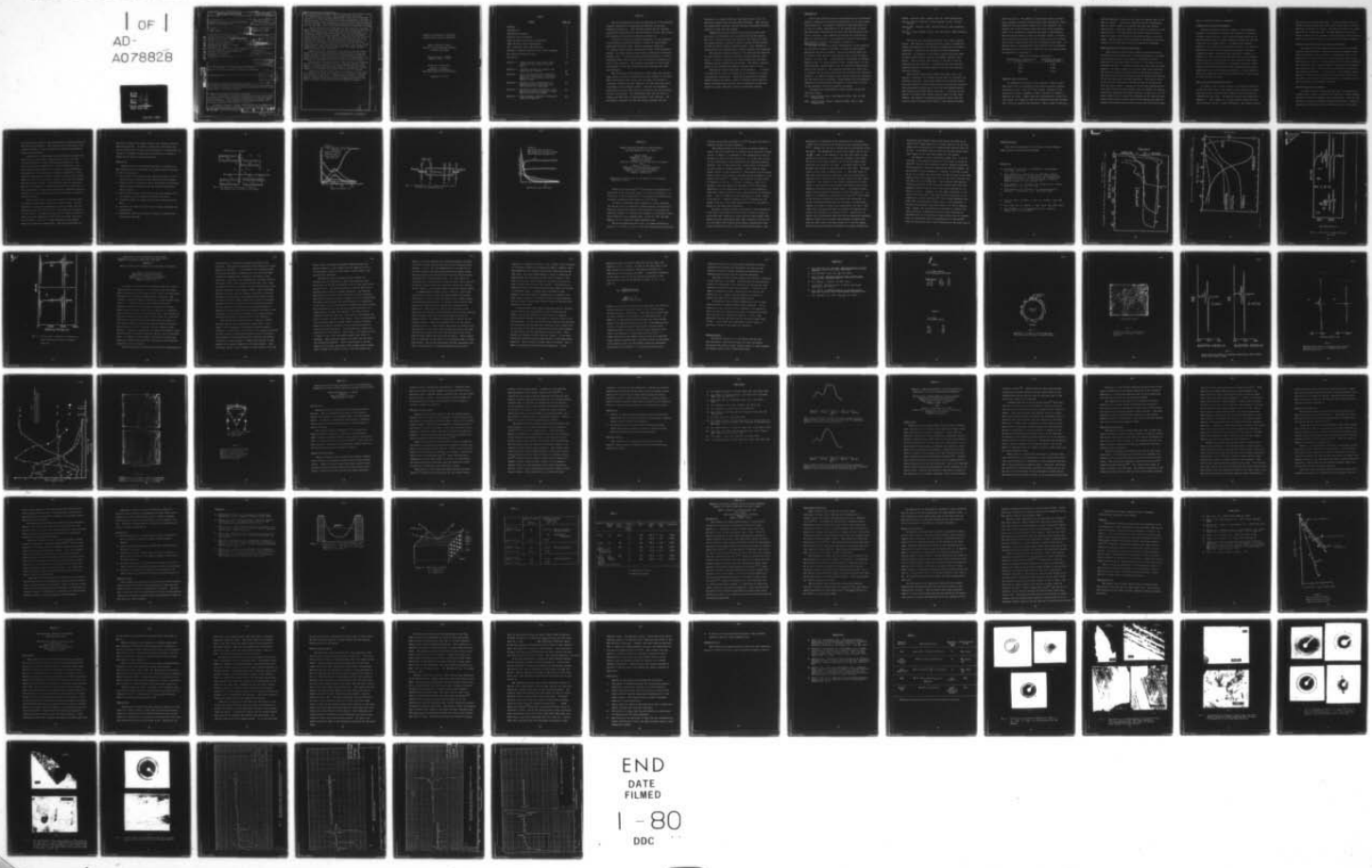

END
DATE
FILMED
1-80
DDC

SECURITY CLASSIFICATION OF THIS PAGE (When Data Entered)

REPORT DOCUMENTATION PAGE

READ INSTRUCTIONS BEFORE COMPLETING FORM

1. REPORT NUMBER	2. GOVT ACCESSION NO.
3. RECIPIENT'S CATALOG NUMBER	
4. TITLE (and Subtitle) Interface Character of Aluminum/Graphite Metal Matrix Composites	5. TYPE OF REPORT & PERIOD COVERED Technical Report Dec. 1, 1977 - Nov. 30, 1979
	6. PERFORMING ORG. REPORT NUMBER
7. AUTHOR(s) Harris, B. L./ Marcus Daniel Lasser	8. CONTRACT OR GRANT NUMBER(s) N 00014-78-C-0094
9. PERFORMING ORGANIZATION NAME AND ADDRESS The University of Texas Dept of Mechanical Engineering/~~Materials Science~~ TAY 167, Austin, TX 78712	10. PROGRAM ELEMENT, PROJECT, TASK AREA & WORK UNIT NUMBERS 031-805
11. CONTROLLING OFFICE NAME AND ADDRESS Office of Naval Research Metallurgy and Ceramics Program Arlington, VA 22217	12. REPORT DATE Dec~~ember 30~~, 1979
	13. NUMBER OF PAGES 82
14. MONITORING AGENCY NAME & ADDRESS(if different from Controlling Office) Dr. B.A. MacDonald, Metallurgy Division Office of Naval Research, Code 471 Department of the Navy Arlington, VA 22217	15. SECURITY CLASS. (of this report) Unclassified
	15a. DECLASSIFICATION/DOWNGRADING SCHEDULE

16. DISTRIBUTION STATEMENT (of this Report)

Technical rept. 1 Dec 77 - 30 Nov 79

DISTRIBUTION STATEMENT A
Approved for public release;
Distribution Unlimited

17. DISTRIBUTION STATEMENT (of the abstract entered in Block 20, if different from Report)

Approved for public release; Distribution unlimited.

18. SUPPLEMENTARY NOTES

19. KEY WORDS (Continue on reverse side if necessary and identify by block number)

Metal Matrix Composites, Al/gr composites, Auger Electron Spectroscopy, Residual Stresses, Interface Characteristics, Electron Loss Spectroscopy, Transverse Strength

20. ABSTRACT (Continue on reverse side if necessary and identify by block number)

One of the problems limiting the application of the aluminum/graphite composites to structural applications is the poor transverse properties. This research program has as a primary purpose the understanding of the contributing factors that govern the transverse strength and methods to improve it.

In order to develop a better understanding of the character of the aluminum/graphite interface, a series of experimental

DD FORM 1 JAN 73 1473 EDITION OF 1 NOV 65 IS OBSOLETE

SECURITY CLASSIFICATION OF THIS PAGE (When Data Entered)

approaches have been used. The key approaches taken are: (1) Scanning Auger Electron Spectroscopy (SAM) of the fractured surface; (2) Auger Spectrum deconvolution techniques to evaluate bonding state; (3) X-ray Residual Stress Measurements; (4) TEM - Interface Phase Identification; and (5) Electronic characterization of the interface. The combined approaches are being used to separate out the many factors that may influence the interface strength.

The SAM results have shown that in most cases the fracture takes place in a region associated with the presence of an oxide. When a deliberate oxide is put onto the fiber an increase in transverse strength had been reported, but only the Al_2O_3 oxide is present on the fracture surface. The role the deliberate oxide coating on the fiber plays in increasing the bond strength is still not defined. The TEM results show that the oxide is γ-Al_2O_3 and that TiB_2 is always present at the interface. The AES results combined with the TEM results indicate that the interface is a complex diffusion zone where the Ti, B, O, Al and other elements form the multilayer structure. What defines the displacement variation and the resulting transverse strength requires a great deal more effort.

Combined AES and CLS spectra using the CLS spectra both as a point of information and to deconvolute the AES spectra has given information about the nature of the bonding in graphite single crystals, carbides, pyrolytic carbon and the surface of high and medium modulus graphite fibers. This information gives promise for characterizing incoming graphite fiber surfaces.

The residual stresses present in the aluminum were measured for two different transverse strength aluminum/graphite composites. No direct correlation is found between the transverse strength and the residual stress pattern. The average residual stress in the aluminum was greater than the yield strength.

Several AES studies were made on the nature of oxide formation and how the inert ion sputtering of an interface can lead to misleading conclusions. Preferential sputtering of weakly bonded elements was noted to lead to different depth profiles. Actual different depth profiles from a segregated surface are noted for oxides containing cations of different valence.

Interface Character of Aluminum/ Graphite Metal Matrix Composites

Annual Technical Report
Office of Naval Research Contract
N 00014-78-C-0094

The University of Texas
Austin, Texas 78712

Principal Investigator

Harris L. Marcus
Mechanical Engineering/
Materials Science and Engineering

December 18, 1979

INDEX

Abstract

One of the problems limiting the application of the aluminum/graphite composites to structural applications is the poor transverse properties. This research program has as a primary purpose the understanding of the contributing factors that govern the transverse strength and methods to improve it.

In order to develop a better understanding of the character of the aluminum/graphite interface, a series of experimental approaches have been used. The key approaches taken are: 1) Scanning Auger Electron Spectroscopy (SAM) of the fractured surface; (2) Auger Spectrum deconvolution techniques to evaluate bonding state; (3) X-ray Residual Stress Measurements; (4) TEM - Interface Phase Identification; and (5) Electronic characterization of the interface. The combined approaches are being used to separate out the many factors that may influence the interface strength.

The SAM results have shown that in most cases the fracture takes place in a region associated with the presence of an oxide. When a deliberate oxide is put onto the fiber an increase in transverse strength had been reported, but only the Al_2O_3 oxide is present on the fracture surface. The role the deliberate oxide coating on the fiber plays in increasing the bond strength is still not defined. The TEM results show that the oxide is γ-Al_2O_3 and that TiB_2 is always present at the interface. The AES results combined with the TEM results indicate that the

interface is a complex diffusion zone where the Ti, B, O, Al and other elements form the multilayer structure. What defines the displacement variation and the resulting transverse strength requires a great deal more effort.

Combined AES and CLS spectra using the CLS spectra both as a point of information and to deconvolute the AES spectra has given information about the nature of the bonding in graphite single crystals, carbides, pyrolytic carbon and the surface of high and medium modulus graphite fibers. This information gives promise for characterizing incoming graphite fiber surfaces.

The residual stresses present in the aluminum were measured for two different transverse strength aluminum/graphite composites. No direct correlation is found between the transverse strength and the residual stress pattern. The average residual stress in the aluminum was greater than the yield strength.

Several AES studies were made on the nature of oxide formation and how the inert ion sputtering of an interface can lead to misleading conclusions. Preferential sputtering of weakly bonded elements was noted to lead to different depth profiles. Actual different depth profiles from a segregated surface are noted for oxides containing cations of different valance.

Introduction

One of the problems limiting the application of the aluminum/graphite composites to structural applications is the poor transverse properties. Development programs of these materials are in need of a basic understanding of the mechanism(s) by which the transverse properties end up lower than that defined by the rule of mixtures. This research program has as a primary purpose the understanding of the contributing factors that govern the transverse strength and methods to improve it.

Experimental Approach

In order to develop a better understanding of the character of the aluminum/graphite interface, a series of experimental approaches have been initiated. The key approaches taken are: 1) Scanning Auger Electron Spectroscopy (SAM) of the fractured surface; (2) Auger Spectrum deconvolution techniques to evaluate bonding state; (3) X-ray Residual Stress Measurements; (4) TEM - Interface Phase Identification; and (5) Electronic characterization of the interface. The combined approaches are being used to separate out the many factors that may influence the interface strength. In addition several other studies related to evaluating the SAM results were performed. These results will be discussed separately and the detailed information in many cases is given in the appendices which are preprints of papers.

The materials investigated in these studies include the following fibers:

T50 - Union Carbide (PAN), High Modulus 393GPa, 3000 or 6000 filaments/tow

T300 - Union Carbide (Rayon), Modulus 230GPa, 1000 or 6000 filaments/tow

HM3000 - Hercules (PAN), Modulus 366 GPa, 3000 filaments/tow

VSB-32, VSB-32-T, VSB-32-0 - Union Carbide (Pitch), 379 GPa 313-13F

Celion 6000 - Celanese (PAN), 241 GPa Modulus, 6000 filaments/ tow

VSO-054 - Union Carbide (Pitch), 500 CPa Modulus, 2000 filaments/ tow

The fibers are infiltrated with the 201 or 6061 aluminum alloys. The materials investigated have a range of mechanical properties depending on the methods of preparation and thermal treatments. These will be discussed for each measurement described. In addition to the fibers, studies have been made on small natural single crystals of graphite obtained from marble. These crystals were examined in the SAM to get the characteristic AES spectrum. In addition they were used for aluminum/graphite interface studies in the TEM and electronic interface studies.

The combined experimental efforts are being used in an attempt to separate out the many factors that may influence the interface strength. Since there seemed to be a strong indication that having an oxide at the interface improved the strength, the thermodynamic properties of the oxide and carbide formers were looked into and are shown in Figure 1. This type of plot assists in defining what oxides could be useful on the fiber. Ideally, the composite transverse properties should obey the rule-of mixtures provided that there is good adhesion between

fiber and matrix. The adherent oxide coating seems to inhibit Al_4C_3 formation and thus prevents undue fiber degradation (hence enhancing the longitudinal properties of the composite) and induces some bonding between fiber and matrix which manifests itself in an increase in transverse strength of the composite. The anticipated chemical nature of the bond, Figure 1, is never truly realized since atoms from the Al alloy melt act to reduce the original oxide coating and form an aluminum oxide layer. To date the superior organometallic oxide coating from a transverse strength point of view is SiO_2, with TiO_2 and ZrO_2 falling short of expectations (see table).

(Data from Aerospace Corporation)

Organometallic Oxide Coating on VSB-32 Fiber	Transverse Strength of Composite Plate
SiO_2	5 ksi
TiO_2	4 ksi
ZrO_2	2 ksi

Scanning Auger Microscopy

To establish the nature of the interface, Scanning Auger Microscopy (SAM) is performed on the aluminum/graphite samples fractured in situ in the 10^{-10} torr vacuum. Details of the approach are given in Appendix B where fractures of composite surfaces are shown. Fibers that were organometallic coated with SiO_2 result in a composite that has increased transverse strength but no SiO_2 is found at the interface. What is seen is the Al_2O_3

and the displaced Ti and B as you inert ion sputter back to the matrix, Figure 2. This can be explained by the thermodynamic data of Figure 1 where it is easily seen that the reaction $4Al(L)+3SiO_2 \rightarrow 2Al_2O_3+3Si$ where the Si goes into solution in the aluminum alloy. Why the use of the initial coating of SiO_2 seems to lead to the increased transverse strength is not yet known. The SAM studies have continued to demonstrate the significance of an oxide layer along the fiber/matrix interface.

Auger Spectrum Deconvolution Techniques

Using spectrum deconvolution computer programs obtained originally from the Sandia and Oak Ridge Laboratories, an effort is in progress to see if any specific information can be obtained from the Auger spectra specific to the nature of the interface bonding. To accomplish this, you start with the Auger spectra. The matrix effect on the Auger peaks associated with the electron escaping from the solid is obtained by measuring the energy loss spectra associated with the primary electron beam of the same energy as the Auger electrons. This matrix effect as well as the instrumental effects can then be deconvoluted from the Auger signal. Integration of the peaks represents the true Auger electron density spectra from the element in question. A series of standards for carbon, carbides, oxides, etc. are now being studied to get a basis for interpreting the interface data. Subtle differences have been noted in the carbide peak behavior between high modulus fibers that do and do not form strong bonds.

This is discussed further in Appendix C.

X-Ray Residual Stress Measurements

Another potential source of a change in the transverse strength of the composite would be the presence of different residual stress patterns. The residual stresses arise due to the large difference in thermal expansion between the oriented fibers and the aluminum matrix. To measure the residual stresses a joint effort was performed with Prof. J.B. Cohen of Northwestern using his ONR developed approaches to measure residual stresses. The results are described in detail in Appendix D. Very little difference was found in the residual stress pattern in the aluminum for two composites where there was a factor of two difference in transverse strength. These initial results indicate that residual stresses may not play a significant role in the transverse strength. Further measurements are planned on an x-ray diffractometer being modified here at the University of Texas.

TEM - Interface Phase Identification

In order to get a direct measure of the crystal structure of the interface layers, the composites were thinned by etching away the aluminum such that the interface layer was partially loosened from the fiber. The detailed results are presented in Appendix F. For a sample of a single graphite fiber/aluminum, the diffraction pattern indexes as γ-Al_2O_3. SAM studies confirm

the presence of the aluminum oxide. In other samples from the regular composites where the oxide was not found the Ti-B region was found to be made up of TiB_2. The TiB_2 was found in all cases where the Ti process was used. The TEM measurements give the direct evidence for the interface crystallography and the results are being evaluated relative to the transverse fracture behavior.

Electronic Characterization of the Gr/Al Interface

The objective of this approach was to see if the interface could be characterized by a change in electrical behavior such that the interface is not destroyed. The approach taken is to measure the I-V characteristics of the composites using a geometry shown in Figure 3. An interesting result has been obtained. The resistance of the material seems to decrease as you lengthen the conducting path. This can only be explainable in terms of the interface character. To pursue this in more depth a system capable of studying the differentiated I-V curve is being built and theory now available in the semiconductor literature will be used to evaluate the interface character.

AES Technique Related Studies

In order to apply combined AES and inert ion sputtering in a quantitative manner to evaluate the interface, several aspects of general sputtering behavior were investigated. The first was related to getting a standard thickness oxide layer. Appendix A describes the AES depth profile associated with a Ti-Mo alloy

and relates the profile to the electrochemical effects associated with the oxide formation. The titanium was investigated to get a known thickness of oxide to assist in determining sputtering rates at the interface.

A second set of experiments were performed to evaluate the possibility of preferential sputtering in a thin interface giving distorted thin layer thickness determinations. The study focused on the segregation to grain boundaries in low alloy steels where elements like Sn and Ni were segregated to the interface. The results are reported in Appendix E. They show that although the apparent Ni profile shows a much thicker layer than the Sn at the grain boundary, the actual thicknesses are most likely the same. The difference seems to be an artifact of the sputtering. This emphasizes the fact that even in thin layer inert ion sputtering preferential sputtering can play a major role if the local bonding for each element is significantly different.

A third study done jointly with Kingery of MIT was aimed at evaluating the sputter profiles of mixed oxides. The purpose was to measure the elemental profile for oxides like MgO containing ions like Ca^{+2} and Sc^{+1} to evaluate the segregation to the surface. An example of the inert ion sputter profile is given in Figure 4 showing the Ca^{+2} to be much more localized at the surface. The Li^{+1} is less localized at the surface where the segregation takes place. The charge difference can

be used to explain this deeper profile since charge neutrality must be maintained. In order to ensure that the profile was not an artifact due to preferential sputtering, as discussed previously, a homogeneous sample was fractured and no change in chemistry was observed during sputtering.

Conclusions

Although none of the research described is complete, we have made progress in evaluating the graphite matrix interface in the following ways.

1. The concept of the oxide at the interface playing a role in the transverse strength has been reenforced and extended.
2. Chemical bonding information about the bonding in the interface by careful analysis of the AES and CLS spectra has been obtained.
3. The residual stress in the aluminum has been measured and no correlation with transverse strength was found.
4. Interface phases of oxides and TiB_2 were identified using TEM.
5. An electrical means of probing the interface character was investigated.
6. Experiments relating quantitative aspects of sputter profiling were reported.

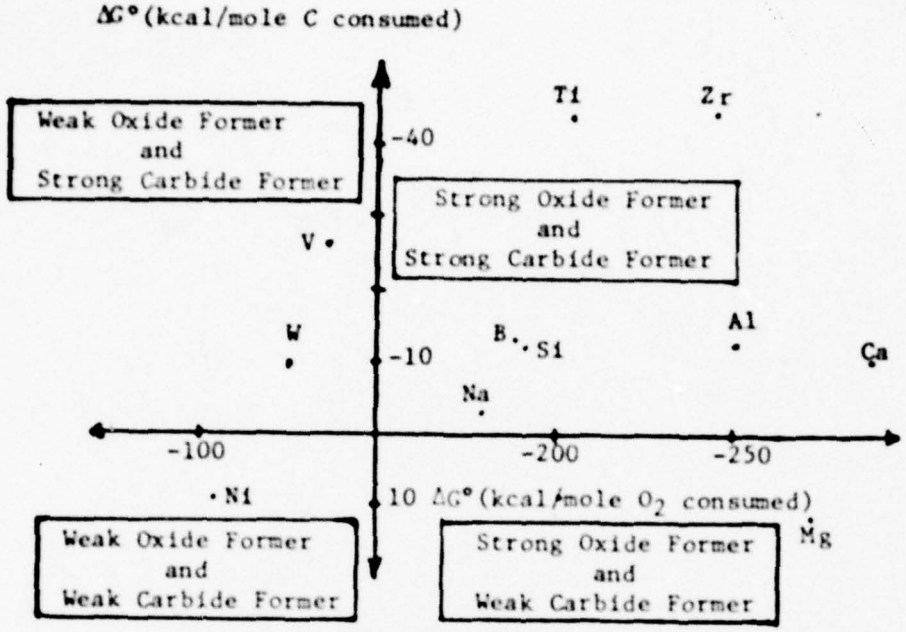

Fig. 1 Room Temperature Free Energies of Formation for Stablest Oxide and Carbide of Each Element

Figure 2:
G 4209 VSB-32-0 (SiO_2)(S)/
6061(Ti+B)
Relative Surface
Concentration vs.
Depth Sputtered
into Matrix

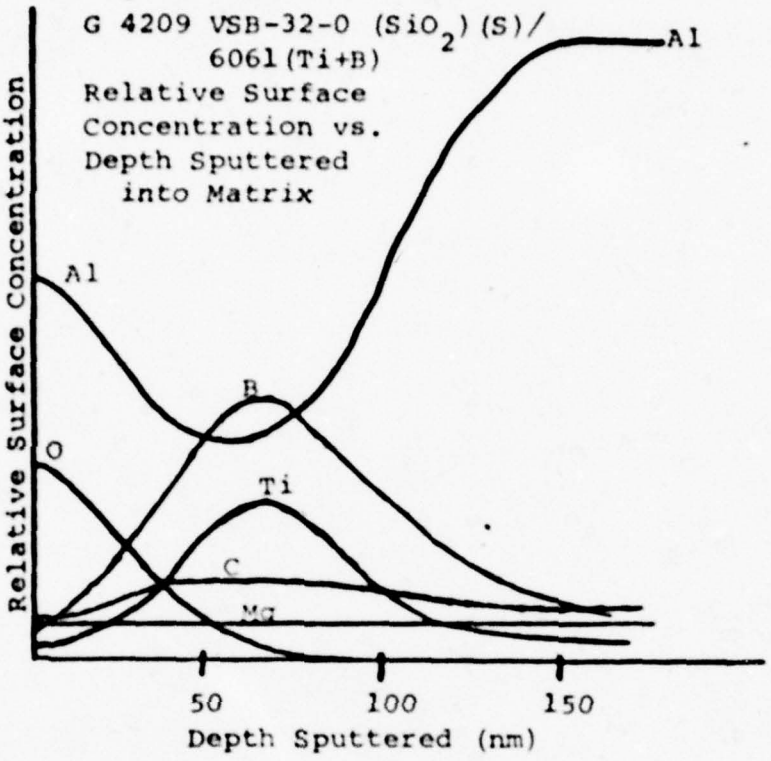

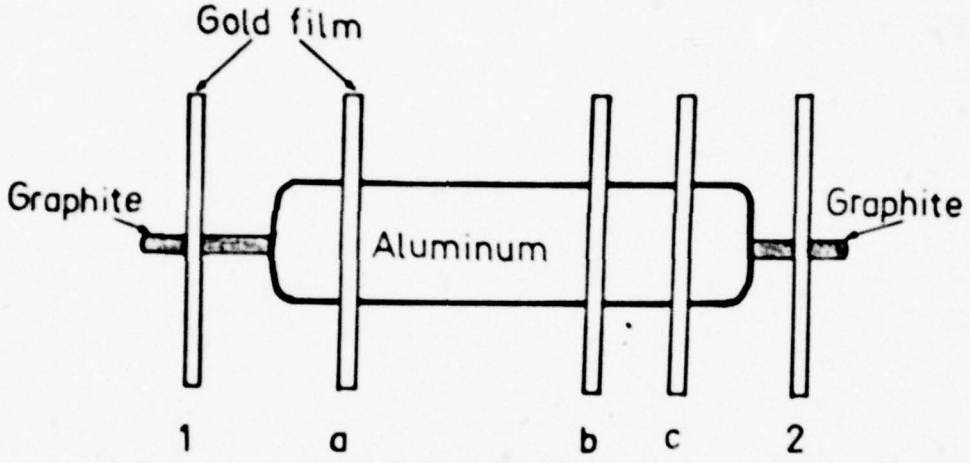

Fig. 3 Configuration of electric contacts used in electronic characterization

Figure 4

MgO Doped with Ca and Sc
AES Depth Profile into Surface
which Exhibits Segregation

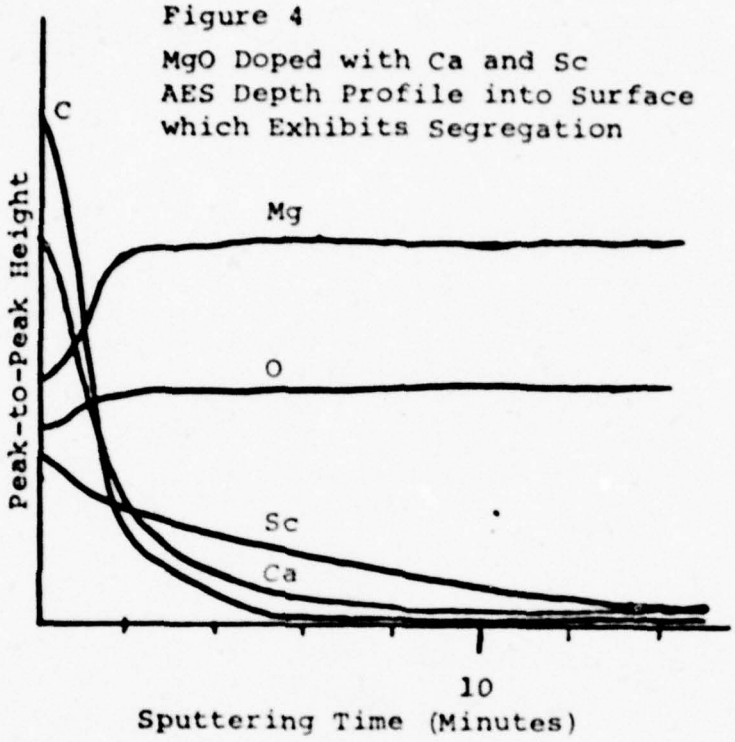

APPENDIX A

"AUGER ELECTRON SPECTROSCOPY DEPTH PROFILE OF THIN OXIDE ON A Ti-Mo ALLOY"

Daniel Laser
Department of Chemistry
Tel-Aviv University
Ramat Aviv, Israel
(Visiting Scientist at the University of Texas)
and
Harris L. Marcus
Department of Mechanical Engineering/
Materials Science and Engineering
University of Texas at Austin
Austin, Texas 78712

(Accepted for publication in the Journal of the Electrochemical Society.)

Recently we investigated [1] the growth and properties of thin oxide films which were grown on a titanium electrode. It is the aim of this communication to describe some properties of an anodic oxide which were grown on a Ti-Mo alloy.

To form a controlled oxide thickness on a bare substrate for use as an AES ion sputtering standard sample, the previously described method was employed which consists of polishing the electrode surface (3μ diamond dust embedded in a polishing cloth) while holding it at a cathodic bias (-0.95V vs. SCE) and then applying to it a positive linear potential scan.

The alloy studied was the β-III, a Ti based metastable β alloy (Ti - 11.5 Mo - 4.5 Sn - 6 Zr) the stress-corrosion behavior

of which was studied by Hickman et al[2] and which was used as received without any heat treatment.

The current/potential curve during the anodic potential scan of the alloy electrode in slightly acidic solution is shown in Fig. 1, where it is compared to the voltammogram of pure Ti and pure Mo under the same conditions. As in the case of pure Ti the voltammogram is distinguished by an extended potential interval (72V) in which the anodic current which is attributed to oxide formation remains constant. Such a mode of oxide growth results in the formation of a homogeneous film the thickness of which varies linearly with the applied potential at full current efficiency.[1] However, the "dissolution peak" which is observed at pure Ti ($\approx$ -0.65V) is missing. This is in agreement with the findings of Tomashov et al[3] who find a suppression in the dissolution rate of Ti at the prepassive state when alloyed with Mo in the β phase and will be discussed later. Little is nown about the composition of anodic oxides of alloyed Ti. Recently Poleolog et al[4] assumed that the anodic oxide of a Ti-Ni alloy consists mainly of TiO_2 with Ni doping at the metal/oxide interface.

We adopt a similar picture with regard to the distribution of Mo within the oxide of the β-III and in order to probe it the oxides were subjected to Auger Electron Spectroscopy (AES) depth profiling immediately after their formation with the use of a PHI Model 590A Scanning Auger system equipped with sputtering, multiplexing and in situ fracturing facilities. The

difficulties in quantitative AES application to very thin (<100Å) TiO_2 films and to Mo oxides have been described before [5,6]. However our aim was to locate the Mo distribution within the oxide. The appearance of the Mo major peaks (186,221 ev in the $\frac{dN}{dE}$ • mode) in the absence of the 27ev peak which is characteristic of metallic Ti, proves the existence of Mo within the oxide if the escape depth of the 27 and 221(186)ev Auger electrons are assumed to be equal. The escape depth of the Mo peaks should even be less than the Ti 27ev peaks. The depth profile of the oxide is shown in Fig. 2. The outer layer of the oxide (oxide/solution interface) consists exclusively of TiO_2 and the Mo concentration increases toward the metal oxide interface. The increase in the carbon concentration in this region is attributed to the polishing procedure prior to film formation (polishing with diamond dust). It should be noted that a similar apparent distribution of Mo can result if: (a) there is a preferential sputtering of Ti over Mo[7] which leads to the surface accumulation of Mo during the sputtering, or (b) Mo is gradually reduced by the ion beam; or continuously changes its oxidation state while penetrating the film in such a way that its Auger peak shape is changed and enhanced even without any increase in its concentration. Possibility (a) should also be manifested after the film is completely sputtered through; however the Mo signal then reaches a steady state. Also the Auger peak of Mo oxide grown at 1 V did not change during the sputtering which eliminates the second possibility.

We believe the chemical state of Mo within the oxide to be that of Mo^{+3} which because of its size, does not fit the TiO_2 phase and thus exhibits in it a much slower mobility than the Ti ion. It probably does not reach the solution/oxide interface except in the very early stages of film growth.

The absence of the Ti dissolution peaks (Fig. 1) may be relevant to the superior behavior of this alloy in corrosive media[2] when the bare substrate might be exposed to solution. Two explanations, which are supported by the AES findings, can be provided to this observation. Firstly, in the AES or pure Mo or of its oxide, the 22lev peaks is smaller than in the 186ev peak but the 22lev Auger peak of Mo in the alloy is bigger than the 186ev one (in the $\frac{dN}{dE}$ mode). This reflects some specific interaction between Ti and Mo in the alloyed state which may possibly stabilize the Ti atom in the solid compared to its state in pure Ti. Secondly, at -0%V while polishing, Ti dissolves into solution[1], but this electrode potential is too negative for the Mo dissolution[8] and it seems therefore feasible that the substrate surface prior to film formation is enriched with Mo which provides a barrier for the Ti dissolution. Indeed, the concentration of Mo which if found by AES after the oxide is removed by sputtering and which may be representative of its quantity at the surface prior to anodization, is much higher than its concentration at the surface hich was obtained by the in situ fracturing of the alloy (Fig.4).

Acknowledgements:

This work was supported by the Office of Naval Research under contract number N00014-78-C-0094.

References:

1. D. Laser, M. Yaniv and S. Gottesfeld, J. Electrochem. Soc., 125, 358 (1978).

2. B.S. Hickman, H.L. Marcus and J.C. Williams, "Stress Corrosion Cracking of Titanium Alloys in Methanolic and Aqueous Environments," Proceedings of the International Symposium on Stress Corrosion Mechanisms in Titanium Alloys, Atlanta, Georgia, January 1971.

3. N.D. Tomashov, G.P. Chernova, Y.S. Ruscal and G.A. Aguyon, Electrochim. Acta., 19, 159 (1974).

4. E.N. Poleolog, A.Z. Fedotova, O.G. Derjagina and N.D. Tomashov, J. Electrochem. Soc., 125, 1410 (1978).

5.

6. T.T. Lin and D. Lichtman, J. Vac. Sci. Technol., 15, 1689 (1978).

7. M.L. Tarng and G.K. Wehner, J. Appl. Phys., 43, 2268 (1972).

8. A.A. Pozdeeva, E.I. Antonovskaya and A.M. Sukhotin, Corros. Sci., 6, 149 (1966).

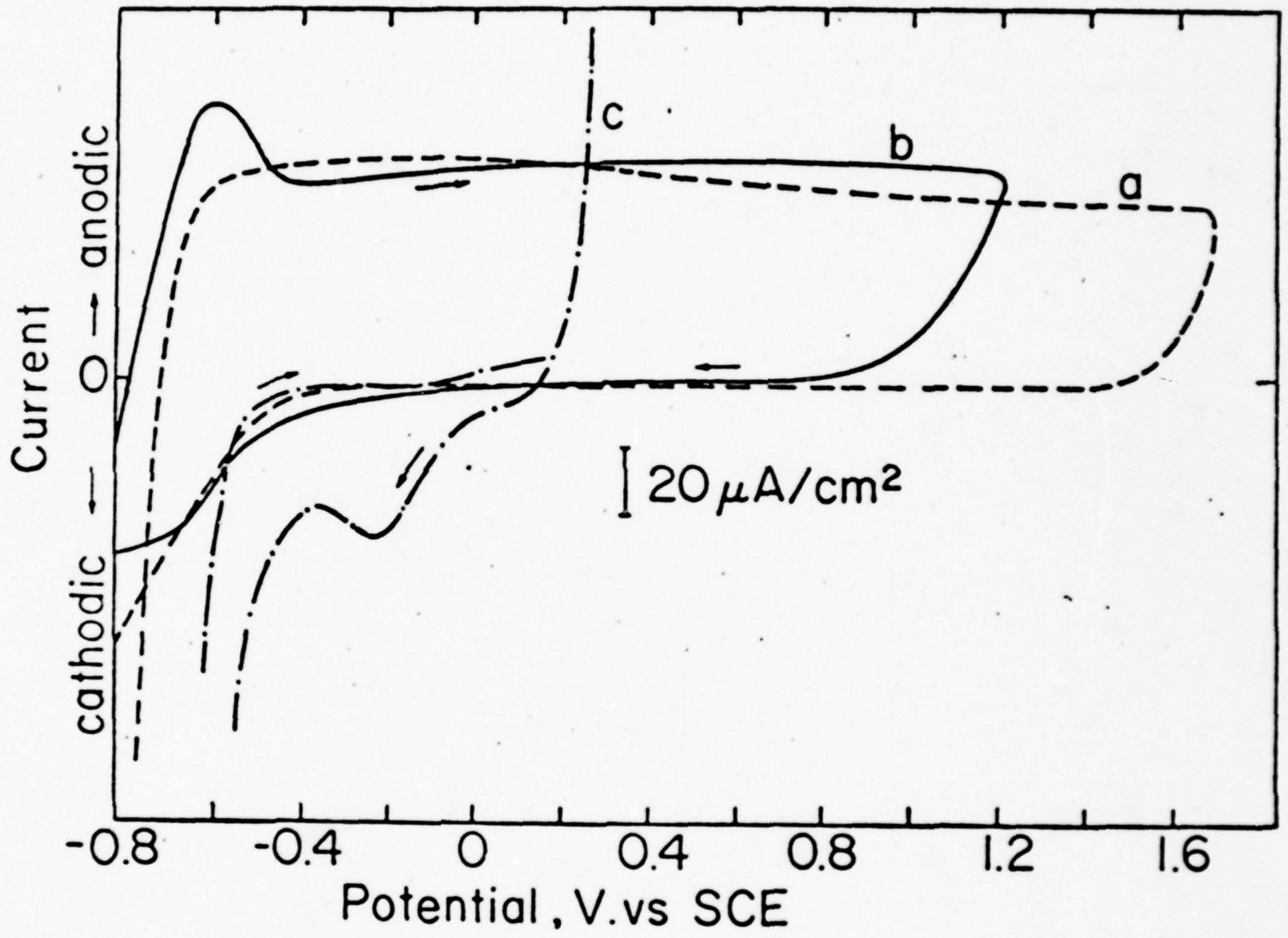

Fig. 1. Current Voltage curve for: β-III alloy (a); Ti (b) and Mo (c). 1N Na_2SO_4, PH = 2.3

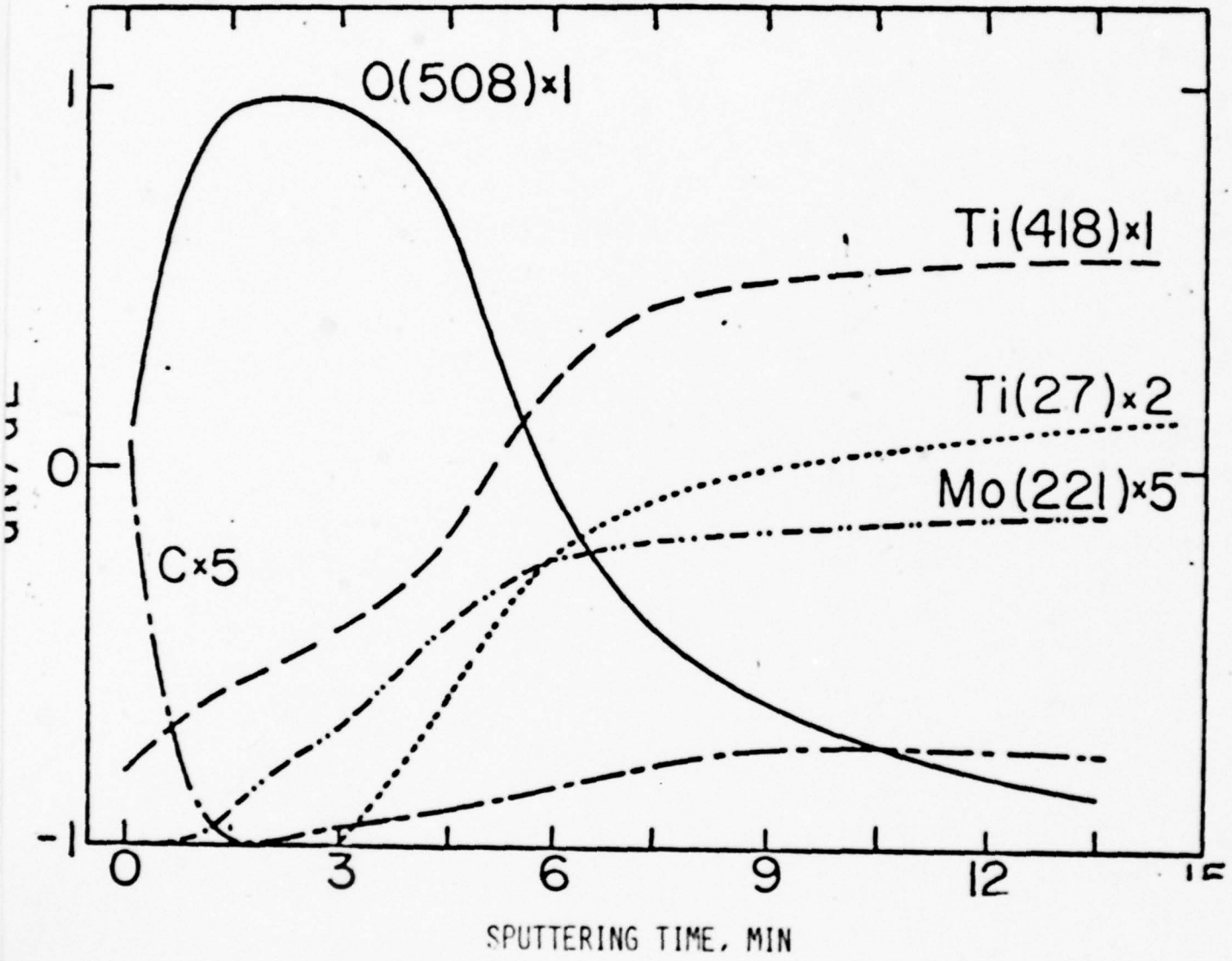

Fig. 2. Depth profile of oxide formed on β-III alloy at 2V, SCE, sputtering by 3KeV Ar^+ ions

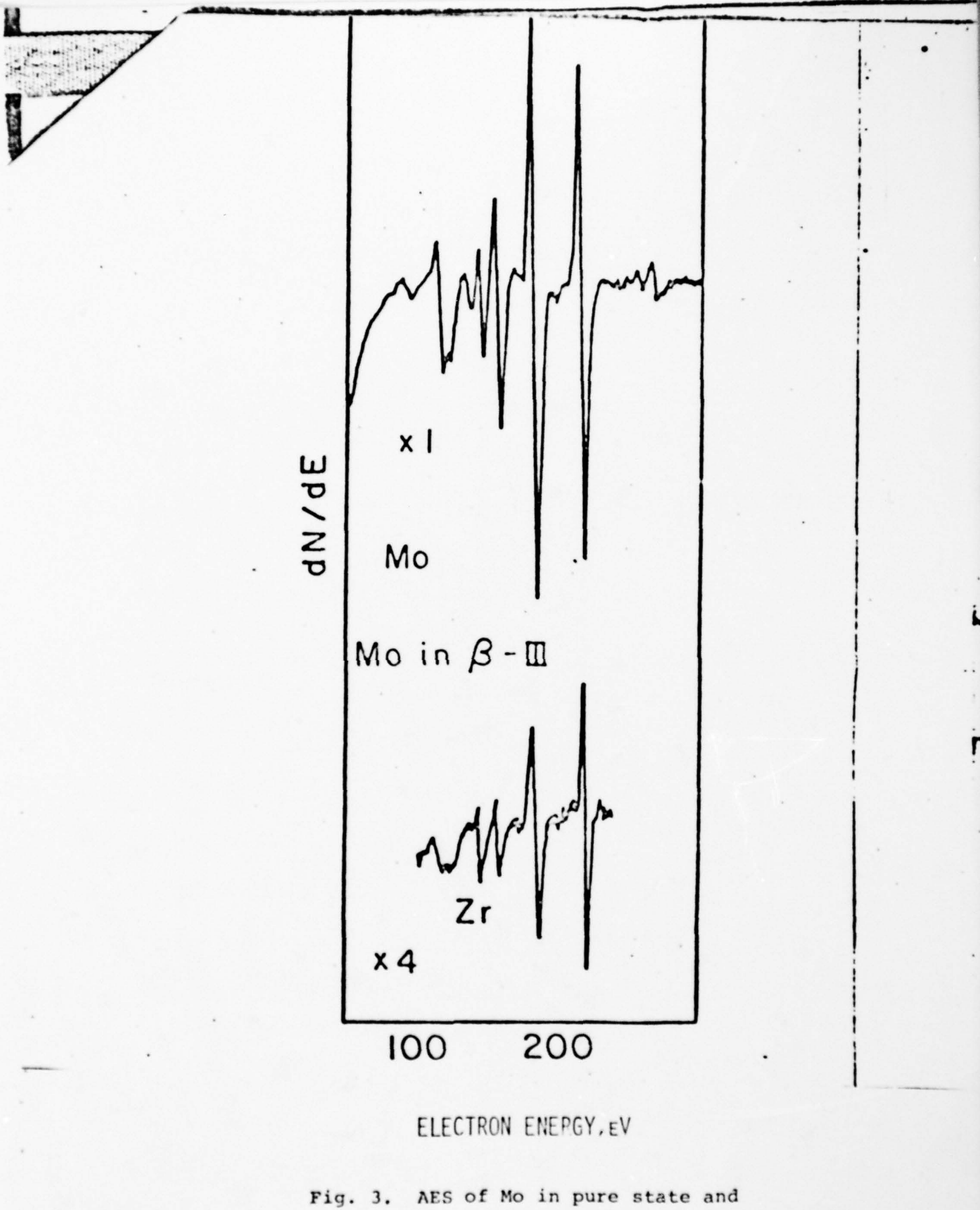

Fig. 3. AES of Mo in pure state and in β-III

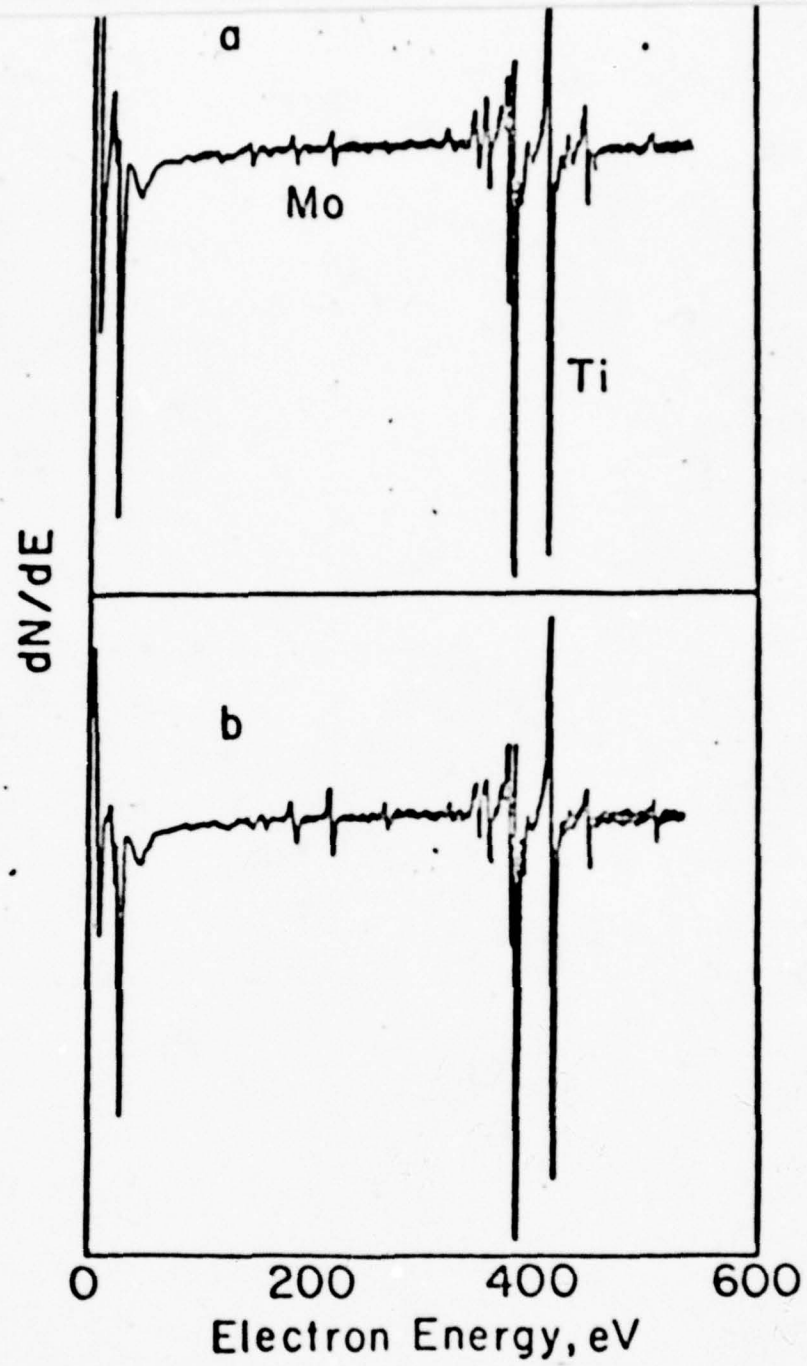

FIG. 4. AES of β-III; fractured in Vacuum (a), after sputtering through the anodic oxide (b).

Published in the Proceedings of the Second Conference on Carbon Fiber Reinforced Metal Matrix Composites, Monterey, California, May 1978

Appendix B

Analytic Methods for Studying the Fiber/Matrix Interface

H.L. Marcus and Duane Finello
Materials Science Laboratories
Department of Mechanical Engineering
The University of Texas at Austin
Austin, Texas 78712

In order to understand the mechanical behavior of metal matrix-graphite composites, it is necessary that the fiber-matrix interface be well characterized. This is of particular importance for transverse loading of the composite. The interface around the graphite composite is shown schematically in Fig. 1. The thickness of the property controlling interface could range from several monolayers in the case where impurities play a major role, to about 0.5 micrometers in the case of a thick carbide reaction zone. The information that an investigator would like to obtain about the interface includes the chemistry across the interface, the nature of the chemical bonding and its influence on fracture strength, the homogeneity of the interface, and the residual stress pattern. (Techniques appropriate for measuring residual stress accurately are not readily available and will not be described here.) In addition, the influence of process variables and subsequent thermal and mechanical treatments on the interface properties would be desired.

The most significant problem associated with characterizing

the interface is directing the measuring probe to the interface. This will be discussed in some detail in a later section of the paper. In this paper we will describe some of the more successful techniques [1] that have been used to make some measurements concerning the nature of the interface. The tools to be discussed are scanning electron microscopy (SEM), Auger electron spectroscopy (AES), inert ion sputtering (IIS), secondary ion mass spectroscopy (SIMS), and ion microprobe mass analysis (IMMA). Other techniques that are evolving, such as scanning transmission electron microscopy and its associated spectroscopic probes as well as lattice imaging in the transmission electron microscope, may very well play a future role in unraveling the nature of the interface. Forming any valid interpretations or descriptive models which define the cohesive strength of the interface will be difficult because of the large chemical and stress gradients in the vicinity of the interface.

The SEM has seen extensive use in composite studies already and will be discussed only briefly here. Fig. 2 shows a SEM micrograph of a fractured aluminum-graphite composite. A major point of interest is the apparent fracture in the vicinity of the graphite-aluminum matrix interface. This exposure of the interface helps alleviate the problem of getting to the interface. Coupled with the SEM in many systems is an energy dispersive x-ray spectrometer. This technique, which is very valuable in bulk analyses, has only

limited value in studying interface chemistry since the chemical analysis is for depths into the samples of 0.5 to 1.0 micrometers, which is most cases is much greater than the interface thickness.

The approach that has shown the most promise in investigating the interface is AES in the scanning mode. The details of AES can be obtained in one of the many review articles [1-5]. The electron beam of a SEM is used as the probing beam to excite the Auger electrons. The electron beam diameter currently being effectively used for detailed AES surface chemical analysis is about 0.2 to 0.5 micrometers. The Auger electrons have the characteristic of originating in the first 0.5 to 2.0 nanometers, depending on their energy. This characteristic allows detailed chemical analysis on a local basis to be made of a surface. The other point of interest is the fact that the local chemical environment can lead to changes in the AES peak shapes. This is particularly true of the AES peak of carbon, where distinctive carbide peaks can be easily separated from the graphite peaks [6] as well as from each other. Similar behavior is shown for many metals in the oxide vs. metal state. An example of this is shown in Fig. 3 for the higher energy Auger peaks of aluminum. The differences between the metal and the oxide are immediately apparent. Much of the change in the AES spectra of the metal comes about from plasmon energy losses. This is shown more clearly in Fig. 4 for the energy loss

spectra of energy analyzed back scattered primary electrons of similar energy interacting with the clean aluminum metal surface. In Fig. 4(a) the characteristic loss spectrum of Al metal displays the peaks associated with plasmon losses, which represent electrons that have given up discrete quanta of energy before leaving the solid. Fig. 4(b) shows the characteristic loss spectrum of aluminum oxide, which exhibits no plasmon losses because the electrons leaving the surface do not undergo a significant amount of discrete energy losses.

A complementary method to AES is the IIS. Inert ions in the 500 to 5000 electron volt range bombard the surface and remove the surface layer by layer as AES of these layers is simultaneously performed. In terms of the interface this allows the chemical profile through the interface to be determined. When fracture occurs in the vicinity of the interface the chemical profiles through the fractured interface can be obtained both into the matrix phase and into the graphite fibers. An example of this type of result for the aluminum-graphite composite sputtered back into the matrix is shown in Fig. 5. This profile shows that the fracture was predominantly in the oxide phase between the matrix and fiber and that the titanium and boron wetting agents used in the process were between the oxide and the matrix. These results will be discussed in more detail in the Amateau paper in these proceedings. One of the significant problems associated with inert ion sputtering of fractured graphite-metal matrix

composites is shadowing effects. Fig. 6 shows a SEM micrograph of a fracture surface of an aluminum-graphite composite and a two-dimensional AES mapping of the argon Auger peak for the same area. The dark regions where no argon is found can be explained by the obstruction of the line of flight of the argon ions by the rough surface not allowing the argon ion beam to reach those parts of the surface. This problem is even more severe for longitudinal fractures where the surface is extremely rough. A second type of problem is that shadowing could also lead to redeposition of elements into other areas, leading to artifacts in the profiling analysis. For this reason, extreme care must be taken in obtaining and evaluating this data.

If the graphite-metal matrix composite does not fracture in the vicinity of the interface, other methods must be used to get at the interface. One method is to sputter through a metallographic cross-section through a fiber to get the interface. If this is done then the relative beam diameter of the probing beam and the fiber diameters play a major role. In the case of the IMMA the appropriate probing beam diameter is the diameter of the focused sputtering ion beam. This diameter is normally greater than two microns. In the case of AES the incident electron beam diameter is the appropriate diameter. This is usually greater than 0.4 microns. Fig. 7 shows a significant problem with this approach. If the

appropriate beam is directed radially with the fiber, the geometry of Fig. 7 occurs. As soon as the outer edge of the beam contacts the interface, the quantity measured is a combination of both matrix and fiber. A geometric evaluation of the relative volume of the interface sputtered in the total volume, shown by the dotted rectangle in Fig. 7, is given by

$$V_R = \frac{\text{interface volume}}{\text{sputtered volume}}$$

$$= \frac{\frac{2\theta\pi}{360}[2R\tau + \tau^2]}{W[R(1 - \cos\theta) + \tau]} \quad .$$

Tables I and II show how both the probing beam size (2R sin θ) and the interface layer thickness, τ, for a fiber radius of three microns, influence V_R. They show that a small beam or large interface is required to get meaningful data. In addition, if the interface has more than one layer, as was shown in the sputtering profiles of Fig. 5 and schematically in Fig. 1, sputtering through the plane of polish would completely mask it since it would be going through all the layers simultaneously, unless they were very thick. A proper analysis of the relative volume would be a layer-by-layer chemical analysis where more detail would be observable in the probing data, but the general conclusion expressed here would not be changed. To accurately determine the

interface thickness using sputtering experiments requires establishing standards for determining the sputter rate. Accurate methods for making standards representative of inhomogeneous material have not yet been developed.

Harrigan [7] has recently reported the results of profiles of the interface using IMMA. The averaging process generally reduced the sharpness of the interface but did provide some elemental information about the interface. In order to use IMMA to determine an oxide, oxygen-18 can be used as the sputtering ion. Oxygen ions are required to assist in making the IMMA profiles somewhat quantitative.

In conclusion, the following observations can be made about probing the graphite-metal matrix interface. If it fractures in the vicinity of the interface, then selective point AES analysis combined with inert ion sputtering allows the interface to be chemically analyzed. If not, then sputtering through the fiber must be done with either IMMA or AES. In all cases the experimenter must be alert to artifacts created by the measuring technique.

Acknowledgement

The authors would like to acknowledge Swe-Den Tsai, Anna Debogorska, and William Slagle for their assistance in getting the profiling data, and the Office of Naval Research for support under contract N00014-78-C-0094.

References

1. P.F. Kane and G.B. Larrabee, Characterization of Solid Surfaces, Plenum Press, New York, 1974.

2. P.H. Holloway, Surf. Sci. 66, 479 (1977).

3. T.A. Carlson, Photoelectron and Auger Spectroscopy, Plenum Press, New York, 1975.

4. H.L. Marcus, J. Metals, 20 (Feb. 1977).

5. J.T. Grant, Characterization of Metal and Polymer Surfaces 1, 133 (1977).

6. C.C. Chang, in Characterization of Solid Surfaces, Kane and Larrabee, eds., Plenum Press, New York, 1974.

7. W.C. Harrigan, Jr., Met. Trans 9A, 503 (1978).

TABLE I

3 μm fiber radius
17 nm interface thickness

Beam Width	2θ	V_R
2 μm	38.6°	.09
0.8 μm	15.0°	.36
0.4 μm	7.5°	.69

TABLE II

2 μm beam
3 μm fiber radius

τnm	V_R
1.7	.01
17.0	.09
51.0	.23

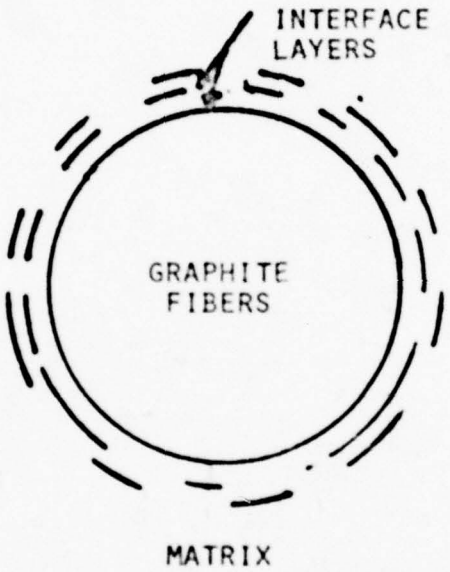

Fig. 1

Schematic of graphite fibers separated from matrix by multiple interface layers

ALUMINUM-GRAPHITE

Fig. 2

Scanning electron micrograph of Al-graphite composite fracture surface

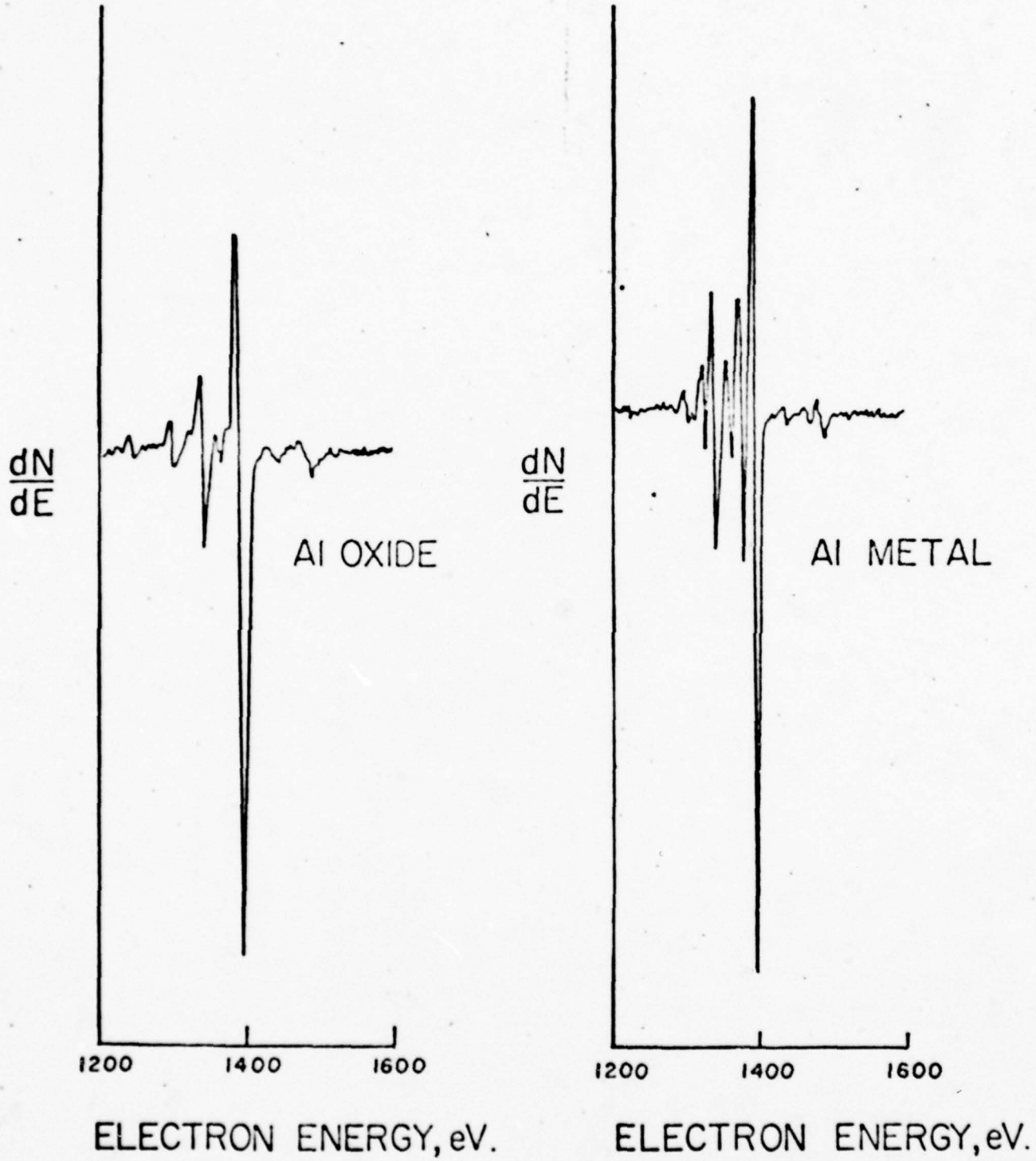

Fig. 3

Auger electron spectra of aluminum showing peak shape change going from oxide to metal

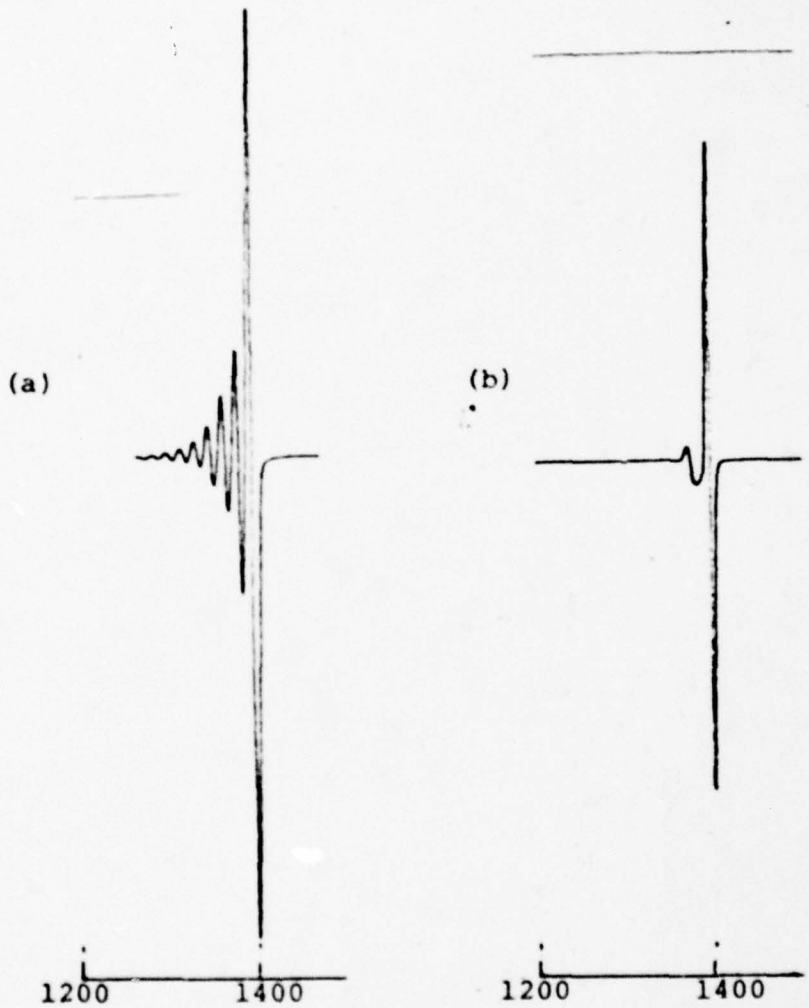

Fig. 4

Characteristic energy loss spectra for 1400 eV primary electrons on (a) aluminum metal and (b) aluminum oxide

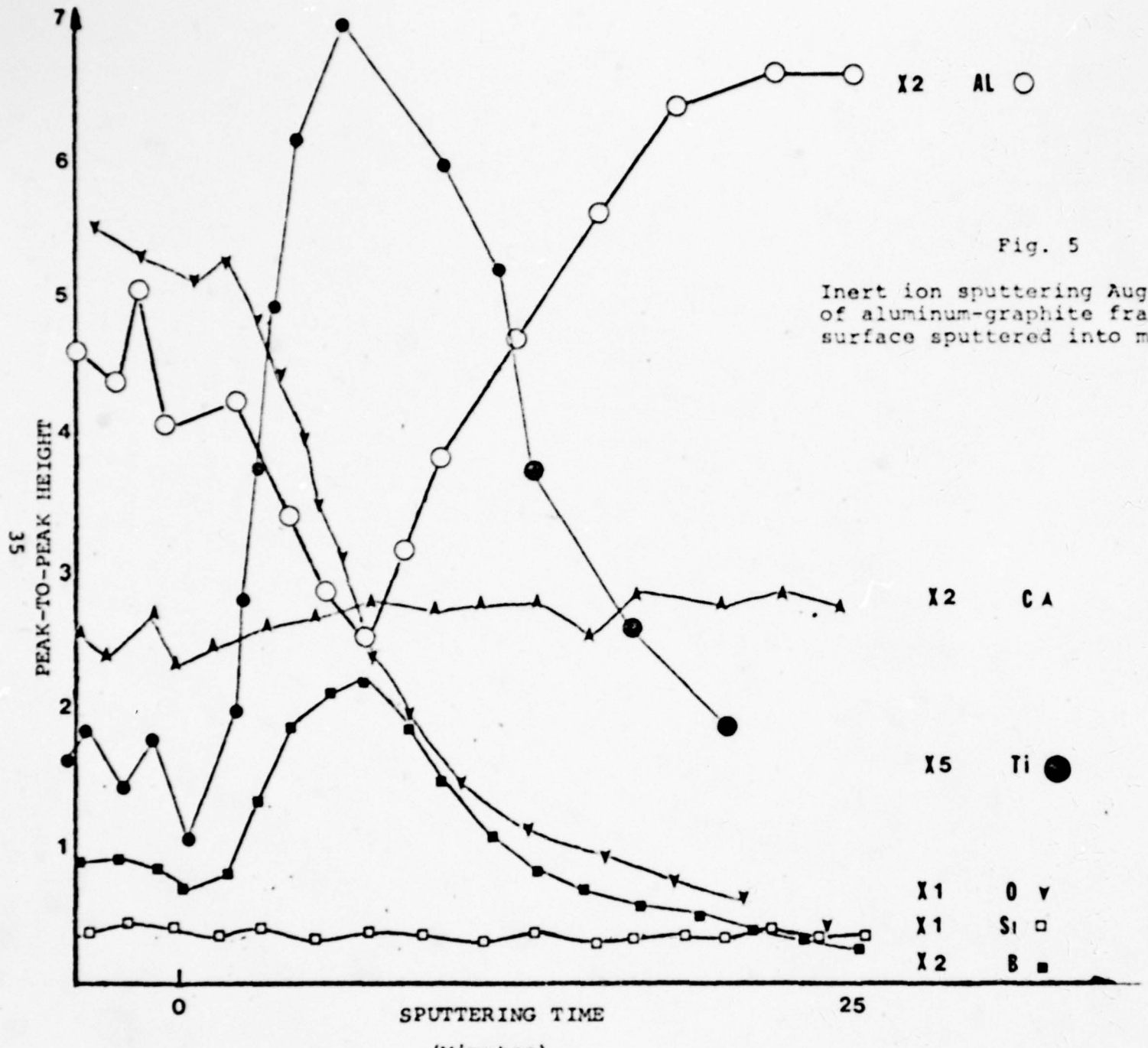

Fig. 5

Inert ion sputtering Auger profile of aluminum-graphite fracture surface sputtered into matrix

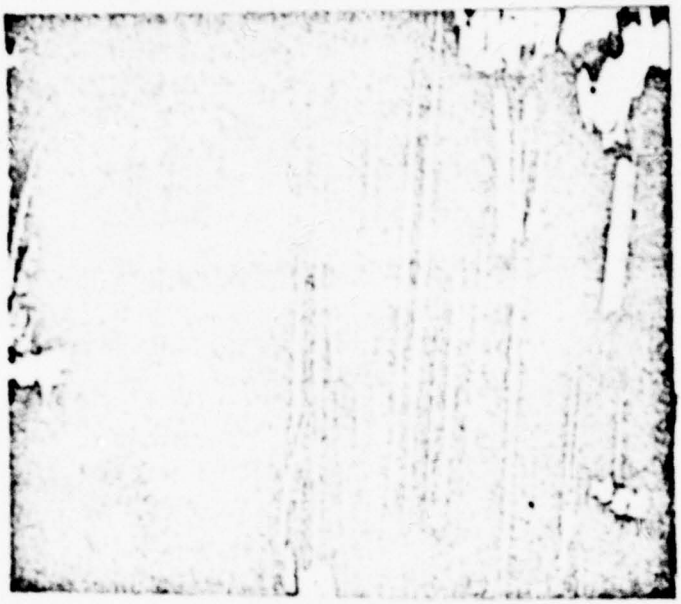

SEM MICROGRAPH

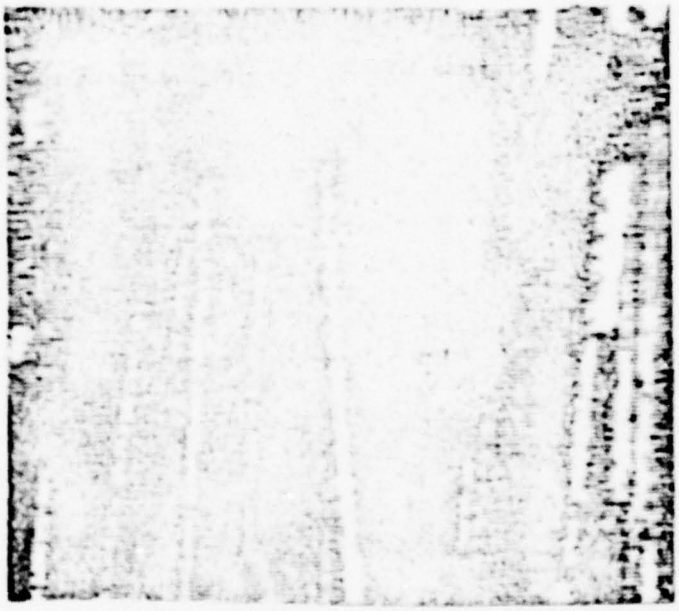

ARGON AES MAPPING

Fig. 6

Implanted Ar Auger map of sputtered aluminum-graphite fracture surface showing shadowing effects and corresponding SEM micrograph

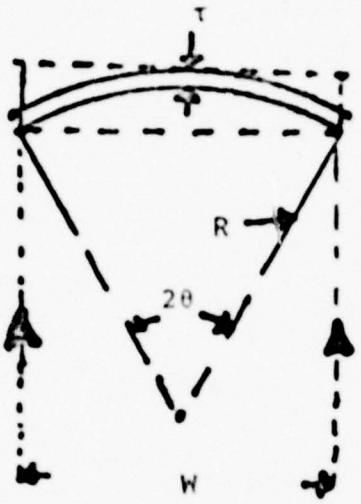

τ - INTERFACE THICKNESS
R - FIBER RADIUS
W - BEAM WIDTH

Fig. 7

Schematic of geometry due to sputtering through plane of polish of graphite-metal matrix composite that leads to averaging of measured interface chemistry

Appendix C

AUGER DECONVOLUTION AND CHARACTERISTIC LOSS SPECTROSCOPIC TECHNIQUES APPLIED TO STUDY CARBON IN VARIOUS BONDING STATES

Duane Finello and H.L. Marcus
ME/MS&E
The University of Texas
Austin, Texas 78712

Introduction

Aluminum/graphite composites have limited transverse strength. This is related to the nature of the bonding between the graphite, the interface layer, and the aluminum alloys. To attempt to understand this behavior, a detailed investigation into the bonding states of various forms of carbon was made.

Use of deconvolution techniques[1-5] to learn more about the bonding orbitals of carbon in various bonding states has been attempted through Auger electron spectroscopy (AES). Characteristic loss spectroscopy[9-12] (CLS) also has been applied to facilitate an alternative analysis which is minimally destructive to the initial surface.

Experimental Procedure

Natural graphite single crystals from marble, graphite fiber material, and pyrolytic carbon were of spectroscopic purity. Graphite single crystal basal plane surfaces were freshly prepared by peeling directly before loading into a Physical Electronics Model 590 scanning Auger microprobe

chamber with no intermediate cleaning step. Graphite fibers were of the Union Carbide Thornel 300 rayon and VSB-32 pitch precursor types. The PVA sizing was burned off them by a 300°C heat treatment in argon. The pyrolytic carbon specimen was a low porocity rod which was fractured in situ to expose a fracture surface for analysis.

Results and Discussion

Results of the deconvolution of the AES spectra are presented (see fig. 1 and 2) for a pyrolytic carbon fracture surface and for a freshly peeled basal plane surface of a graphite single crystal. Not all of the peaked structures derived for the density of states of carbon in the form of single crystal graphite coincide in energy with those obtained for pyrolytic graphite. The peak energies for the pyrolytic graphite came close to those calculated theoretically.[2,6]

There is a significant difference between the experimental density of states for the pyrolytic graphite and the basal plane of the graphite single crystal. There is even more difference when the carbon is present as a carbide, a difference easily seen in the raw AES data.[8] These characteristic fingerprints of the carbon peak can be used in interpreting the aluminum/graphite interface data, but additional effort is required to determine their electronic origin.

The results in both cases are complicated by many-body effects[7] arising from the presence of the K-shell vacancy

created in the Auger process. In addition, some electron beam disruption of the initial surface structure[8] is unavoidable since any local AES technique striving for fine spatial resolution generally requires use of a micron-diameter incident beam of electrons of appreciable current density. It is noteworthy that in the extreme case, the end result of the electron beam damage is to render all carbon surfaces indistinguishable via AES, whether originally graphite single crystal, graphite fiber, or pyrolytic graphite. Experimental care must be taken to minimize this effect.

An alternative way to obtain information concerning surface structure is to utilize characteristic loss spectroscopy[9-12] (CLS) in the integral mode. This structure-sensitive technique is considerably more delicate by virture of the fact that it requires only a small fraction of the electron beam current density and voltage required with AES. The CLS process does not generate core holes; rather, it is intended to probe energy loss mechanisms the incident electrons experience upon interaction with the specimen surface. CLS results suggest that major differences in phonon excitation[3] tendencies exist between a basal plane surface of a graphite single crystal and the surface of a low-modulus graphite fiber of circumferential basal plane orientation. The CLS results can be interpreted in terms of phonon excitation phenomena. This interpretation is currently being

evaluated. As part of this evaluation, a variety of incident electron beam voltages will be used in the CLS studies to see what effect it will have on the relative amount of phonon excitation caused. Based on these results, graphite fibers having different surface basal plane orientations and different degrees of graphitization should be distinguishable via CLS.

Conclusions

1. Density of states of carbon obtained using deconvolution techniques show distinct differences for pyrolytic graphite, single crystal graphite and carbides.
2. CLS results also show significant differences between fibers and single crystals in terms of structure in the spectrum attributable to phonon interactions.

Acknowledgement

This research was supported by the Office of Naval Research under Contract N 00014-78-C-0094 at the University of Texas at Austin.

References

1. H.D. Hagstrum and G.E. Becker, Phys. Rev. B4 (1971) 4187.
2. J.A. Tagle, V. Martinez-Saez, J.M. Rojo and M. Salmeron, Surf. Sci. 79 (1978) 77.
3. M.A. Smith and L.L. Levenson, Phys. Rev. B 16 (1977) 2973.
4. J.E. Houston, J. Vac. Sci. Technol. 12 (1975) 255.
5. C.J. Powell, Sol. State Comm. 26 (1978) 557.
6. R.F. Willis, B. Fitton and G.S. Painter, Phys. Rev. B9 (1974) 1926.
7. M. Cini, Surf. Sci. 87 (1979) 483.
8. C.C. Chang (1974) in "Characterization of Solid Surfaces," P.F. Kane and G.G. Larabee, eds., Chapter 20, Plenum Press, New York.
9. M.L. Knotek and J.E. Houston, Phys. Rev. B 15 (1977), 4580.
10. T.S. Sun, J.M. Chen, R.K. Viswanadham and J.A.S. Green, Appl. Phys. Lett. 31 (1977) 580.
11. J.E. Rowe, J. Vac. Sci. Technol. 13 (1976) 798.
12. J.J. Ritsko and M.J. Rice, Phys. Rev. Lett. 42 (1979) 666.

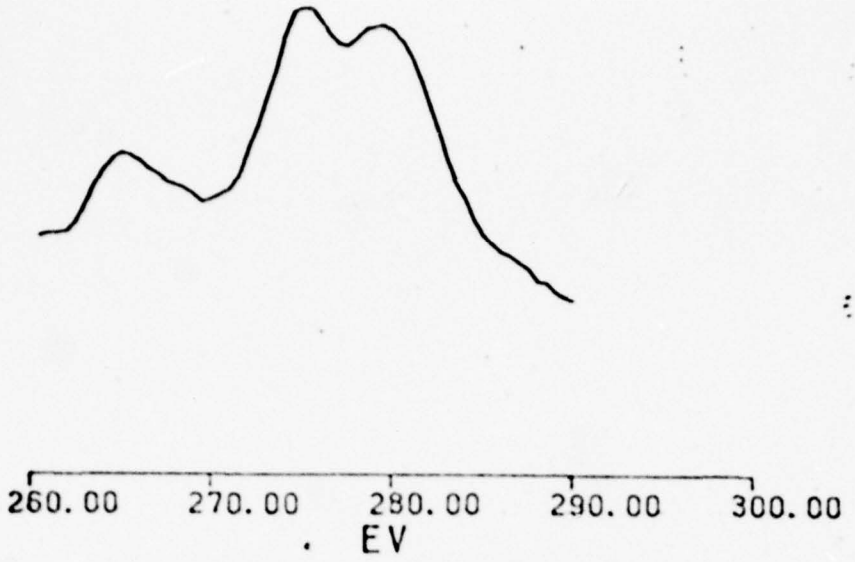

Fig 1. Experimentally derived transition density function representing valence band density of states for pyrolytic graphite with Fermi energy at 285 eV.

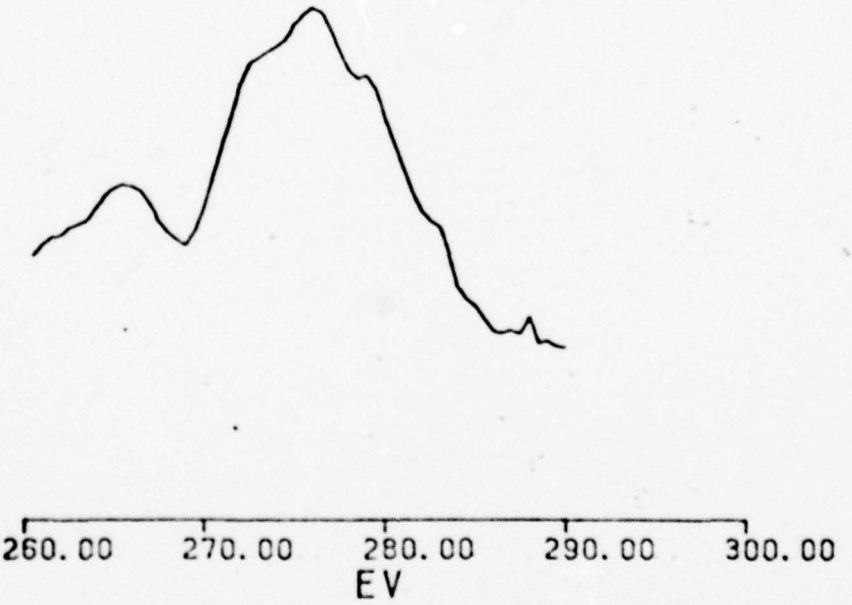

Fig 2. Experimentally derived transition density function representing valence band density of states for single crystal graphite (0001) planes with Fermi energy at 285 eV.

Appendix D

"RESIDUAL STRESS MEASUREMENTS ON ALUMINUM-GRAPHITE COMPOSITES USING X-RAY DIFFRACTION TECHNIQUES"

Swe-Den Tsai, Deepak Mahulikar and H.L. Marcus
Department of Mechanical Engineering/
Materials Science and Engineering
University of Texas at Austin
Austin, Texas 78712

and

Ismail C. Noyan and J.B. Cohen
Department of Materials Science and Engineering
Northwestern University
Evanston, Illinois

INTRODUCTION

Metal Matrix Composites (MMCs) have generated considerable interest in the materials field, because of their potential applications in dynamic structures. A MMC with its excellent mechanical as well as physical properties carries a distinct advantage over other composite systems, particularly at high temperatures. At the same time a MMC system is characterized by heterogeneity, anisotropy and interfaces which affect those properties considerably. Interfaces have been known to influence the properties of MMCs significantly and their importance has been discussed extensively[1]. However, the interface chemistry and its exact role in alteration of various properties is not well-known yet. One of the important things needed for better understanding of the interface is its stress state. Thermal and mechanical treatments involved in the fabrication of composite materials, give rise to triaxial

residual stresses[2]. Speculations are that these stresses, originating from the differing thermal coefficients of the reinforcement and the matrix, play an important part in the transverse properties of the MMCs.

A simple calculation using a planar model[3] shows that stresses well above the yield strength of aluminum exist at the interface of the aluminum-matrix-graphite fiber composite system. This occurs because the graphite fibers are introduced into molten aluminum and during the subsequent cooling, aluminum contracts much more than the graphite in the fiber direction. Plastic flow is expected to occur because of the high values of thermally induced stresses in that direction. Assuming no debonding, a stress gradient is expected in the Al matrix, with above-yield tensile stress at the interface. A schematic of the expected stress distribution in the longitudinal direction is given in Fig. 1. The dotted line represents average value of stress in the aluminum matrix. All of the matrix is expected to be in a state of tensile stress minimized at a point between fibers.

While there is a significant difference in thermal expansion coefficients of Al and graphite in the longitudinal direction, this difference is negligible in the transverse direction due to the anisotropy of graphite fiber. Therefore, the residual stresses in the transverse direction are mechanical in origin due to the development of the longitudinal stress and are not expected to be as high as those in the longitudinal direction.

Cryogenic cooling induces additional plastic flow in the matrix establishing a new elastic condition at the cryogenic temperature. Heating the composite back to room temperature will then relieve much of the residual stresses.

For experimental verification of the above mentioned observations, residual stress measurements are essential. This paper discusses a method of residual stress measurements for composite systems and presents several results. The data obtained is then interpreted with reference to the models described earlier and relative to the finite interface between the aluminum matrix and graphite fiber.

EXPERIMENTAL PROCEDURES

The residual stress measurements were made on three different transverse strength aluminum-graphite composite systems. The nominal properties and the fiber and matrix components of the systems are given in Table 1. The measurements were also made on samples quenched to liquid N_2 temperatures and then tested at room temperature.

The X-ray diffraction technique was used for the stress measurement. The measurements were made on a computer controlled Picker powder diffractometer using parafocussing geometry. This particular technique involved use of the $\sin^2\Psi$ method described elsewhere[4]. Six Ψ angle tilts taken in equal increments were employed. The surface components of the stress were obtained by a computer for a least square straight

liné fit to the lattice strain as a function of $\sin^2\psi$. (Peak positions were determined with an 11 point parabolic fit.) Only those data with a correlation factor of 0.95 and above were considered sufficiently accurate. In order to counteract grain size effect 2θ oscillations of 2 degrees were employed. A cobalt X-ray source of 0.15 cm^2 area was employed; 90 percent of the intensity came from a depth of 5.4×10^{-3} cm. Due to the relatively large divergent beam, the stress measurement obtained was a volume average over the matrix similar to one represented by the dotted line in Fig. 1. For such a volume average, the penetration depth of X-rays becomes an important parameter. Since it is the stress in the vicinity of the interface that is of interest here, it is absolutely essential to expose the interface of the specimen to the X-rays. In other words, the penetration depth should be such that the X-rays average over the region which includes interface.

Mechanical polishing was not used since it could introduce residual stresses. By electropolishing, enough surface could be removed so as to expose the interface area, and to get rid of the surface layer that may have been stressed by mechanical working. For G 3437 and G 3394 the sample surfaces were polished just enough to expose portions of interfaces. With G 3675 only light electrolytic polishing was done. This resulted in a thin surface layer of aluminum above the fibers having thickness greater than the penetration depth of the X-rays used. Thus during volume averaging only the aluminum matrix containing no

fibers would be covered and not the interfacial area. Specimens used were plates with a thickness of approximately 0.4 cm, and 1.9 to 2.5 cm width and length. Residual stress measurements were made in both the longitudinal and transverse direction as indicated in Figure 2.

RESULTS AND DISCUSSION

The residual stresses measured with the 420 diffraction peak of aluminum are listed in Table 2. The table also lists the correlation factors for the least-squares straight line fit for the lattice strain vs $\sin^2\psi$.

It may be noted that the longitudinal fiber stress values for G 3437 and G 3394 are comparable to the yield strength of the 201 aluminum matrix, indicating that the longitudinal interfacial stress is even higher than this average value which was predicted by the simplistic planar model. This also seems to support the presence of plastic flow.

However, in the transverse direction, significant stresses are noted in the G 3437 and G 3394 specimens. In the absence of a significant difference in thermal coefficients of expansion of the matrix and fiber in that direction, one expects the thermal stresses to be much lower than those in the longitudinal direction. The yielding of the aluminum probably gives rise to the observed large residual stresses.

For the G 3675 composite, which was electropolished only slightly with almost no interfacial region exposed, very low

stresses were observed. This was because the X-rays did not include appreciable amounts of the interfacial region below the surface layer of aluminum, and hence no interfacial stress contribution was recorded.

An interesting observation was, that while the transverse fracture strengths of the composites varied (Table 1), the recorded residual stresses varied only slightly. This indicated that the residual stresses may not be affecting transverse strengths to any appreciable extent.

The model described in Fig. 1 did not consider a finite thickness interface. It has been observed[5,6] that an oxide, carbide, or titanium diboride is usually present at the fiber matrix interface in Al-graphite systems. Since the mismatch between the thermal coefficients of the compounds and the aluminum matrix is lower than that of the fiber and the aluminum in the longitudinal direction, the longitudinal residual stresses at the interfaces can be expected to be lower than when an aluminum graphite interface exists. It is the interfacial chemistry which is responsible for a particular mismatch in thermal coefficients.

When the G 3437 composites were quenched in liquid nitrogen and annealed at room temperature, approximately 30% reduction in residual stress was observed. This is less of a reduction than is calculated from the differences in coefficient of thermal expansion. Additional work hardening at the interface occurring during cooling may explain this difference.

Additional research is being conducted to study the residual stress effects in Al-graphite and other metal matrix composites. Higher energy X-rays will be used to increase the penetration depth with a respective rise in averaged volume. Interface chemistry and its influence on transverse properties is under investigation.

CONCLUSIONS

1. X-ray diffraction is an effective procedure for measurement of residual stresses in metal matrix composite systems.
2. Large longitudinal residual stresses were observed in Al-graphite composites.
3. Transverse residual stresses were observed in spite of the limited mismatch in the thermal expansion coefficient in that direction.
4. No large difference in the residual stresses for two different transverse strength Al-graphite systems was measured.
5. Quenching a composite in liquid N_2 and annealing it at room temperature reduced the stresses by approximately 30%.

ACKNOWLEDGEMENT

This research was sponsored by the Office of Naval Research, Contract N 00014-78-C-0094 at the University of Texas and Contract N 00014-75-C-0580 at Northwestern University. The work done in the Long-Term X-ray Diffraction Facility of Northwestern University's Materials Research Center was supported in part by NSF (Grant No. DMR 76-80847).

REFERENCES

1. COMPOSITE MATERIALS, v.1 "Interfaces in Metal Matrix Composites" Ed. A.G. Metcalfe, Academic Press, 1974.

2. Ebert, L.J. and P. Kennard Wright, "Mechanical Aspects of the Interface" in Composite Materials, v.1, ed. A.G. Metcalfe, Academic Press, 1974, p. 53.

3. Hoffman, C.A., (1970) Effects of thermal loading on composites with constituents of differing thermal expansion coefficients. NASA-TN-D 5926.

4. James, M.R. and Cohen, J.B. "Study of the Precision of X-ray Stress Analysis," Adv. in X-ray Analysis 20, 1977 pp. 291-308.

5. Dull, D.L. and Amateau, M.F., Transverse Strength Properties of Graphite-Aluminum Composites, Final Report for Period 1, Oct. 1976 - Sept. 30, 1977; prepared for Naval Surface Weapons Center.

6. Marcus, H.L., Dull, D.L. and Amateau, M.F., "Scanning Auger Analysis of Fracture Surfaces in Graphite-Aluminum Composites," in Failure Modes in Composites IV, J.A. Cornie and F.W. Crossman, eds. Conference Proceedings, The Metallurgical Society of AIME, Fall, 1977.

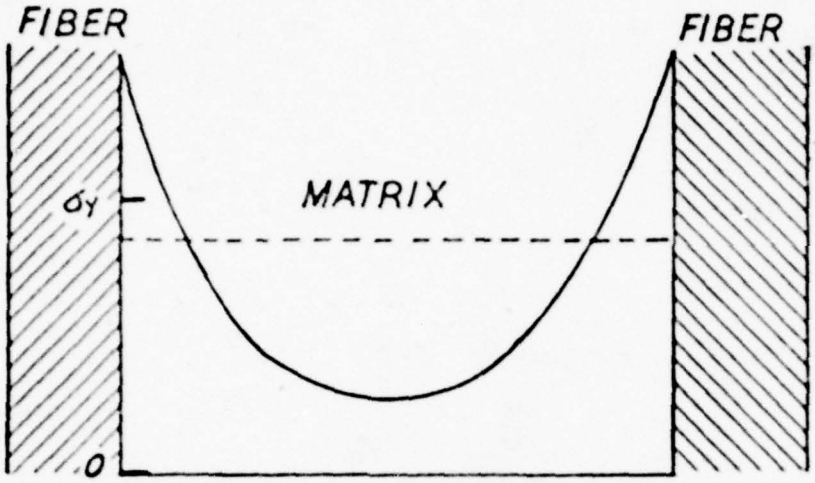

Figure 1. A simple model to show the residual stress distribution. The dotted line is an average value. The term σ_y is the yield strength of the matrix.

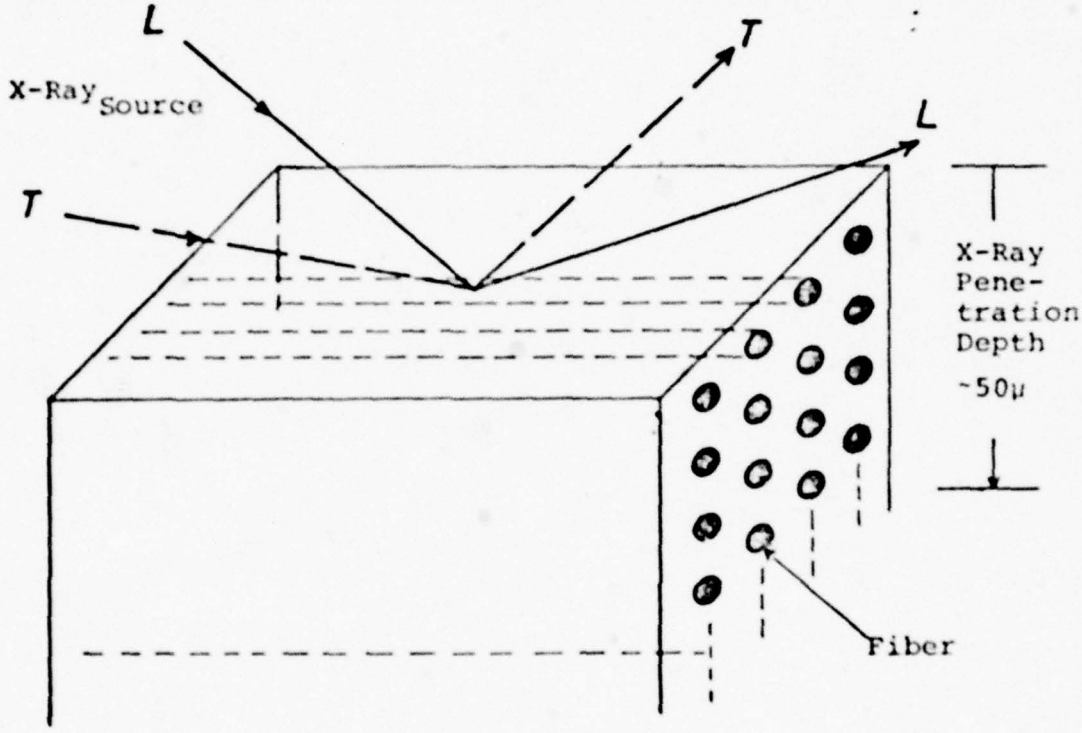

Figure 2. Measurement Geometry

L - Longitudinal

T - Transverse

Table 1

	Young's modulus 10^6 psi	Thermal expansion coefficient 10^{-6} / °C	
Thornel 50 (Fiber in G3394)	60	-0.1~-0.4	(axial direction) to about 300°C
		~25	(transverse direction)
(Matrix Al-201)	10.2	23.22	
Thornel 300 (Fiber in G3437)	35	~-0.23	(axial direction)
(Matrix Al-201)	10.2	23.22	
Celion 6000 (Fiber in G3675)	34	~-0.23	(axial direction)
(Matrix Al-6061)	10.0	23.58	

Table 2

Material	Transverse Strength MPa	Longitudinal Strength	Direction of Measurement Residual Stress	Diffraction Peak	Residual Stress MPa	Statistical Error MPa	Correlation Coefficient
G 3437	10	1120	L	420	199.38	± 3.87	0.9640
			T	420	166.28	± 3.61	0.9658
G 3394	20	763	L	420	228.38	± 1.46	0.9945
G 3675 [Away from the graphite-aluminum interface]	75	259	L	420	40.71	± 0.86	0.9507
			T	420	33.26	± 0.79	0.9788
G 3437 [cooled to liq. N_2 temp and measured at room temperature]	10 (before quench)	1120	L	420	144.11	± 2.55	0.9856
			T	420	120.20	± 2.25	0.9924

L = Longitudinal direction

T = Transverse direction

Appendix E

ANOMALOUS SPUTTERING EFFECTS IN THE AES GRAIN BOUNDARY ANALYSIS OF TEMPER EMBRITTLED LOW ALLOY STEELS

Michael Schmerling, Duane Finello and
H.L. Marcus
The University of Texas at Austin
ME/MS&E
Austin, Texas 78712

Introduction

The mechanism of temper embrittlement in alloy steels involves the segregation of alloying elements to grain boundaries. Diffusion of these elements occurs over long periods of time in the embrittling range (~350 - 525°C) or may be accelerated to occur within 200 hours by cooling in "steps" through this range. The embrittling process consists of an increase in the ductile-to-brittle transition temperature and can be reversed by annealing for several minutes at temperatures above 600°C.[1] The segregation of elements such as Ni, Sn, Sb, P, and other metalloids to prior austenite grain boundaries was confirmed using AES.[2,3] Inert ion sputtering (using incident ions of from 0.5 to 5 keV energy) in conjunction with surface analysis by Auger electron spectroscopy allows depth profiles of elemental concentration to be taken.[2,4] These profiles indicate that most embrittling alloying elements are concentrated in thin layers (~.5 to 1 nm) at the boundaries, but that Ni segregation appears in a somewhat thicker layer (1-3 nm).[2,4] Possible explanations for this difference are 1 - actual difference in depth; 2 - difference in sputtering rates resulting in selective sputtering. Since artifacts due to preferential sputtering are often encountered when depth profiles are made, it is necessary to check the profiles against a standard preparation.

Experimental Procedure

Step-cooled brittle alloys of a Ni-Cr-Sn steel (35 wt%Ni, 1.7% Cr, .3% C, .06% Sn) were fractured in a scanning Auger microscope (PHI SAM 590 system) at a vacuum of 1.3×10^{-8} Pa. To reduce the likelihood of shadowing during sputtering of the rough surface, two ion guns aimed from opposite directions were used. At approximately 500x magnification, grains were selected for analysis on a basis of facet orientation. A facet suitable for the analysis had to serve as a broad target for electron and ion beams as well. The chamber was backfilled with argon to 4×10^{-3} Pa. The electron beam position was fixed for the duration of each sputtering profile to maintain the spatial resolution below 5000 nm. Sputtering was performed with both ion guns at 4 keV and 2 $\mu A/cm^2$ ion current.

The fractured specimen was then moved from in front of the Auger analyzer to a position under a Ni filament. The filament was resistively heated in order to deposit a quantity of Ni so as to duplicate the concentration characteristic of the as-fractured surface, as evidenced by the Ni-Fe peak height ratio. The specimen was repositioned and a new sputter profile was taken at the same point as on the original profile. This was repeated for different deposition times.

The conversion from sputter time to depth of material removed is based on sputter rates of Ta_2O_5 with the same experimental parameters for the sputter guns. The actual depths can be different, as this work shows.

An exponential fit was used for obtaining a layer thickness from the sputtering data consistent with Ta_2O_5 sputter rates. A true exponential decay would occur only if the rate of Ni concentration change were directly proportional to the amount of Ni on the surface in the form of a partial monolayer.

Results and Discussion

The profiles obtained showed roughly an exponential decay in the concentration of Ni and Sn which implies that sputtering removes each constituent at a rate which is approximately proportional to the quantity present at the surface at any given time. From the semilogarithmic plot of the elemental concentrations of Sn and Ni versus depth sputtered (Fig. 1) it appears that Sn is removed via sputtering in a different way than Ni. One may define a time constant τ as the sputtering time required for the surface concentration of the segregated element to reach 1/e of the difference between the original surface concentration and the bulk concentration which is assumed to be the steady state surface concentration ultimately achieved during sputtering. For Ni, τ can be seen (Fig. 1) to be approximately twice that of Sn. All sputtering was continued until the bulk concentrations were seen.

For the series of Ni deposition experiments the sputter profile data had approximately the same time constant as the segregated Ni profile. The conclusion from these experiments that Ni is less readily sputtered than Sn depends on the assumption that the coverage by deposition of Ni is a replica of the

original segregate distribution on the fracture surface. Replication was attempted by using Ni deposition to restore the Ni-Fe peak height ratio to its original value.

The most likely morphology for Ni deposition on a facet of the grain would be a partial monolayer since the Ni-Fe signal ratio was found to be approximately a linear function of deposition time for the small quantities of Ni deposited. This would not be true for multilayered island growth. The fact that both the starting concentrations and the apparent depth profiles are the same implies that the Ni segregation results in approximately the same morphology. If the coverage is kept to less than a monolayer, the finite escape depth of the Auger electrons or the backscattering factor would not influence the sputtering results.

Various models have been proposed to explain the apparent long-range segregation of Ni in comparison to other segregating elements in low alloy steels.[4,5,6,7] Precipitates of Ni-rich regions at carbide-ferrite boundaries or other locations would explain the depth of Ni but this account appears to be inconsistent with the present duplication of the rate of sputtering following deposition. The large Sn atoms are more weakly bound to the matrix of smaller Fe atoms than are the Ni atoms, which are extremely close in size and structure to the Fe atoms. The fact that Cr (again similar to Fe and Ni) has been reported possibly to have a "longer" segregation range[6] may also be an artifact due to stronger bonding and corresponding lower sputtering rate. Specimens quenched during various stages of embrittlement show Ni concentrations reaching a maximum away from the fracture surface, which is not the case after complete embrittlement.[6]

No attempt was made to duplicate these incomplete embrittlement profiles in this study.

Summary

The present research indicates that the morphology of the Ni segregated to grain boundaries in the low alloy steel exists over a thickness of approximately a monolayer in depth at the surface. The Ni segregation kinetics indicate a partial monolayer grain boundary morphology; the exact morphology could be investigated further by studying elastic reflection intensities.[8] Perhaps Ni is strongly bonded to the grain and is therefore relatively difficult to remove with inert ion sputtering. The resulting slower sputter rate of the segregated Ni provides an explanation for the seemingly deeper concentration enrichment and degree of Ni segregation suggested by experiments involving AES in conjunction with IIS for low alloy steels.

Work is now being undertaken with deposition in vacuum of both Ni and Sn partial monolayers onto a previously sputtered embrittled steel grain. The sputter profile of these layers will be a further check on the present results.

Acknowledgements

The authors wish to thank General Electric Research and Development Laboratory for the steel alloy used. This research was sponsored by the Office of Naval Research, Contract N 00014-78-C-0094.

REFERENCES

1. Low, J.R., Jr., (1969) Trans AIME 245, 2481.

2. Marcus, H.L. and Palmberg, P.W. (1969) Trans AIME 245, 1664.

3. Stein, D.F., Joshi, A. and LaForce, R.P., (1969) ASM Trans Q. 62, 776.

4. Marcus, H.L., Hackett, L.H. Jr., and Palmberg, P.W. (1972) Temper Embrittlement of Alloy Steels, ASTM STP 499, 90.

5. Smith, C.L., and Low, J.R. (1974) Met Trans 5 279.

6. Joshi, A. and Stein, D.F. (1972) ASTM STP 499, 59.

7. "Application of Auger Electron Spectroscopy in Ferrous Metallurgy," by L. Marchut and C.J. McMahon Jr., in Electron and Positron Spectroscopies in Materials Science and Engineering, O. Buck, J.K. Tien and H.L. Marcus, Eds., New York: Academic Press, 1979.

8. Seah, M.P. (1973) Surface Sci 40, p. 595.

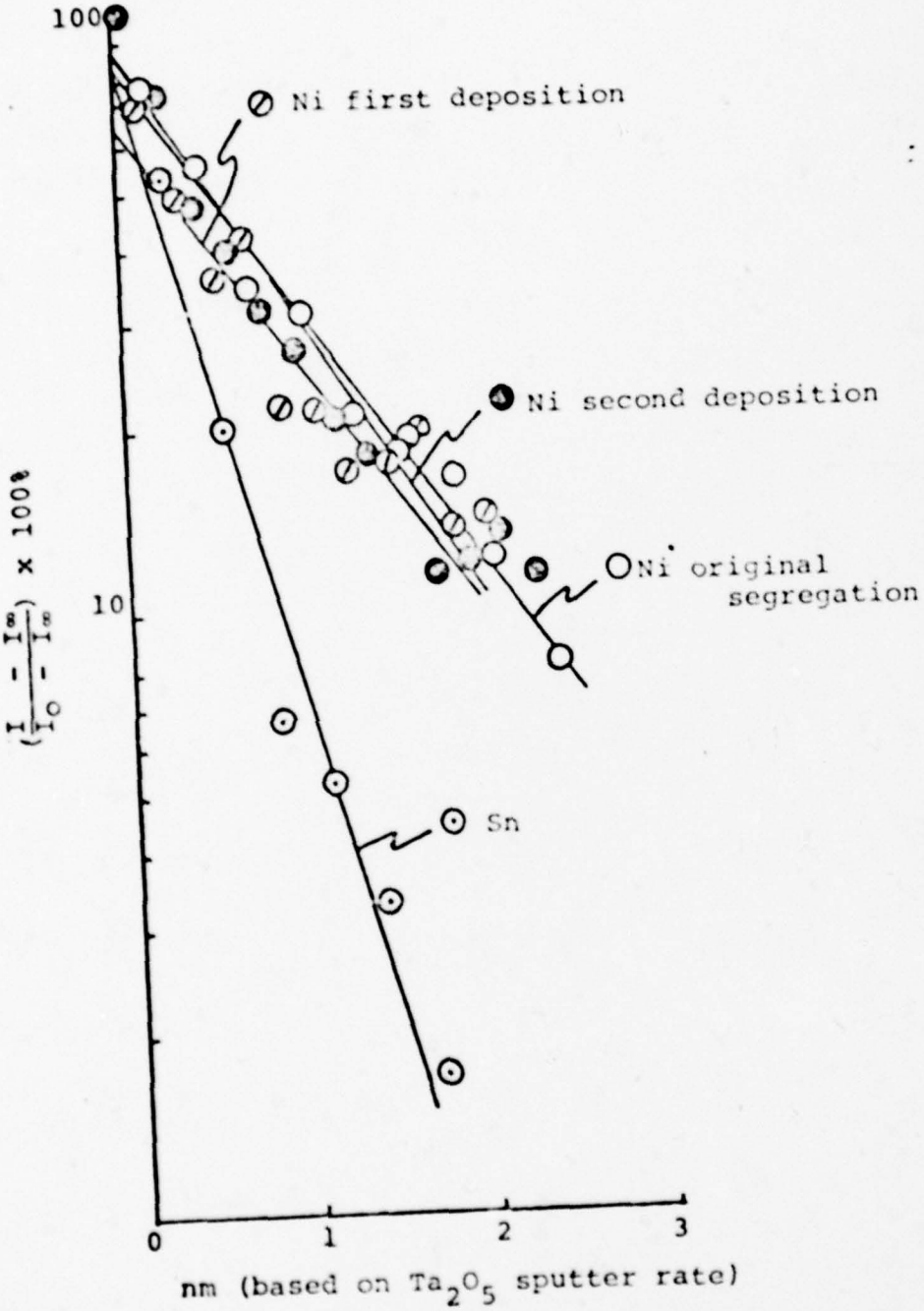

Figure 1
Ni, Sn sputter profile
(lines through data points
are least squares fit)

Appendix F

THE INTERFACE STRUCTURE IN GRAPHITE/ ALUMINUM COMPOSITES

Swe-Den Tsai, Michael Schmerling and
H.L. Marcus
Mechanical Engineering/
Materials Science and Engineering
The University of Texas
Austin, TX 78712

Introduction

The graphite fiber reinforcement/metal matrix composites are of great interest because of their high strength and the potential for larger-scale production. Aluminum alloys appear promising as matrix materials for graphite reinforced metal. However, a pretreatment or coating layer for graphite fiber is needed to promote the wettability between the fiber and aluminum matrix. For instance, a technique for fabrication of this composite has been developed by applying a chemical vapor deposited Ti/B layer (Ti/B CVD) coating to the surface of the graphite fiber followed by controlled immersion into molten aluminum.[1] The resultant Ti/B coating exhibits a sufficiently low contact angle so as to provide rapid and complete infiltration. Even as this liquid metal infiltration technology became more mature, the transverse strength of graphite-aluminum composite remained poor in contrast to the high strength in longitudinal direction. A recent study[1] indicated that the interfacial properties should be closely related to the transverse behavior. This interface could be the reaction zone between aluminum and fiber

or the reaction zone between coating and either the fiber or matrix.

Some variations in the treatment of graphite fiber have been developing,[2] such as the modification of Ti/B CVD or use of a porcelain enamel coating process prior to the standard Ti/B CVD process to improve the transverse strength. But the basic understanding about the crystal structure of the interface phases is still lacking.

The aim of the present work was to obtain crystallographic information about the interface reaction zone through electron diffraction using TEM. The corresponding interface chemistry on some specimens was also studied by using a Scanning Auger Microscope (SAM). Various composite materials with different transverse strengths were employed in order to correlate the structure of interface phase with mechanical properties.

Titanium diboride (TiB_2) was found in the interface layer near to the graphite fiber for every material processed by the standard Ti/B CVD. Aluminum oxide - $Al_2O_3\gamma$ phase was also observed in most materials studied here.

Experimental

The graphite/aluminum composite materials examined in this study are listed in Table 1 along with the processing method, transverse strength and the interface phases observed in TEM. Except for G3842 which is the plate consolidated from T133 wire, the other materials are all precursor wires. Basically, two

fiber types were involved here, each representing currently available commercial forms. The Celion 6000 is low modulus type II PAN fiber with the graphite basal plane parallel to the fiber surface. The VSB-32 and HM3000 are high modulus pitch type fiber with basal plane perpendicular to the surface. All fibers have circular cross sections.

To make the fiber-matrix interface accessible to observation, a selective etching method was used. The materials were dipped or swabbed in various etchants, concentrated HCl solution, HCl solution diluted by 60~70% volume percent methanol or 7N KOH solution. The samples were then thoroughly rinsed with acetone, methanol or ultrasonically cleaned in the methanol. Thus, the sample fibers were free of the aluminum matrix material and only some interface pieces in the neighborhood of the fiber surface were left. Searching around the fiber surface revealed numerous interface pieces thin enough for electron transmission in the samples prepared in HCl solution diluted by methanol or in concentrated HCl solution. Some thin interface layers also were found in the sample etched by KOH.

Both the composite wire and plate were fractured in situ in the SAM under 10^{-10} Torr vacuum in order to unambiguously analyze the material in the fractured interface region between fiber and matrix. In addition, some of the ion etched samples were examined to identify the chemical species present. An electron beam spot size of approximately 1μ or less was used

to give good spatial resolution and high signal to noise ratio. The SAM instrument applied in these studies was the Physical Electronics model 590 system.

Results and Discussion

The most often observed phase was a TiB_2 hexagonal structure which was found in all materials studied here. This type of interfacial layer was found extending from the surface of the fibers. Several larger pieces were about the size of fiber radius and curved along the shapes of the fiber circumference. Some typical electron diffraction patterns of TiB_2 prepared in HCl plus methanol for various composite materials are shown in Fig. 1. The observation of the spotty nature of the rings in the diffraction pattern of T114A indicated that the grain size of TiB_2 in the T114A composite was larger than the grain size of TiB_2 in the other composites studied here. This grain size difference was consistently observed in many fibers and also in samples prepared by some other selective etchants, like concentrated HCl or KOH. One basic difference between T114A and the rest of the composite materials is that the Celion 6000 fiber in T114 has the graphite basal plane parallel to the fiber surface but the other composites have the pitch type fiber with basal plane perpendicular to the surface. This difference of crystallographic orientation in the substrate may offer a preferential growth for TiB_2 reaction product. The grain size effect may play a role in the transverse properties of the composites.

A close investigation into the morphology of the TiB_2 layer in electron micrographs for various composites showed some striated characteristics (see Fig. 2) of this interface layer in pitch fiber reinforced materials. This situation is possibly correlated to the orientation of basal plane mentioned above. The comparison between pitch and non-pitch fiber composites can be seen in Fig. 2 and Fig. 3, where the TiB_2 phase with striated crenulation for VSB-32, HM3000 pitch type composites (Fig. 2) and without for Celion 6000 PAN II type composites (Fig. 3) are presented. Here the diffraction pattern of Fig. 2 (c, d) is shown in Fig. (b) ahd that of Fig. 3 is shown in Fig. 1 (c).

Another significant result in this work was the observation of an aluminum oxide (Al_2O_3) phase along the fiber/matrix interface. The origin of the oxide has not been clearly established, but it is most likely the reaction product of oxygen contained in fibers segregated to the interface during the aluminum-infiltration processing step. The exact role of this oxide layer is not known at present, but the recent SAM studies[4] indicate that it seems to promote matrix adhesion to the graphite and might be favorable for a better transverse strength in graphite/aluminum composites. The present careful TEM examination of these oxide layers on the fiber surfaces indicated that the Al_2O_3 phase has relatively larger grain size on the average than that of TiB_2. The electron diffraction patterns of Al_2O_3

(Fig. 4) were observed only in T114A, G3842, T105A composites. In T105A composites, a mixture of Al_2O_3 and TiB_2 was also found (see Fig. 4 (d). The relatively continuous nature of the TiB_2 portion of diffraction ring implied it has a smaller grain size than that of Al_2O_3 in this mixture. The coexistence of Al_2O_3 and TiB_2 was also identified in Auger electron spectroscopy which will be discussed later. (Fig.5 shows the morphology of Fig.4(b).)

It is also interesting to point out that titanium carbide, TiC was observed in G3842 and T105A composites. In both materials, the rings of diffraction pattern are continuous, however the diffraction ring is broadened to some extent in T105A composite. This is believed to be due to the effect of very fine grain size. The diffraction pattern and micrograph can be seen in Fig. 6.

The interface reaction zone in the composites studied in TEM was also investigated by SAM to help identify the chemistry. Interesting results were found in the fractured samples. The fracture paths were through the oxide layer or close to either the fiber side or matrix side of the interfaces. The Auger spectrum versus the depth from fracture surface was obtained using the inert argon ion sputtering experiment. Using sensitivity factors[5] estimation of the concentration ratio of titanium to boron, Ti/B at the selected points after sputtering were consistently about 0.51-0.57 in the plate G3636 made from T105A and in the plate G3842 made from T133 (see Fig. 7 and 8). This ratio confirmed that the TiB_2 phase was present in the

interface layer. The spectrum in Fig. 7 shows this ratio along with the presence of aluminum oxide, discussed previously in the TEM diffraction patterns. However, the Auger electron spectrum, Fig. 9, taken from T114A precursor wire gave the relatively low Ti/B ratio of approximately 0.2~0.28. (The standard TiB_2 SAM spectra is shown in Figure 10.) Assuming titanium boride is stoichiometric TiB_2, this ratio may include boron in other borides with the elements present or possibly in a complex $(TiAl)B_2$ type boride. Further studies are being conducted in the TEM and SAM to clarify and extend the results reported in this paper.

Conclusions

Results of this work can be summarized as follows:

1. TiB_2 phase is generally present for the aluminum/graphite composites processed by standard Ti-B CVD technology.
2. Larger TiB_2 phase grain size was observed in Celion 6000 fiber with the graphite basal plane perpendicular to the fiber surface. This could relate to higher transverse strength in T114A composites.
3. $Al_2O_3\gamma$ phase was found in some composites and is relatively larger in grain size than the TiB_2 phase.
4. The mixture of $Al_2O_3\gamma$ and TiB_2 was observed in some areas of interface for the T105A composite.
5. AES identified the existence of TiB_2 with the stoichiometric atomic concentration ratio, for many interface areas in most composites studied.

6. A smaller Ti/B ratio from AES appeared in the interface reaction layer for T114A composite wire.

Acknowledgement

This research was sponsored by the Office of Naval Research, Contract N 00014-78-C-0094 at the University of Texas at Austin.

References

1. Dull, D.L. and Amateau, M.F., "Transverse Strength Properties of Graphite-Aluminum Composites," Quarterly Progress Report No. 1, TOR-0077 (2726-03)-1, The Aerospace Corporation, El Segundo, CA, (10 Jan, 1977).

2. Steckel, G.L, Flowers, R.H. and Amateau, M.F., "Transverse Strength Properties of Graphite-Aluminum Composites," Final Report for Period 1 Oct. 1977 - 30 Sept. 1978 for Naval Surface Weapons Center, TOR-0078 (3726-03)-4, Sept. 30, 1978.

3. Amateau, M.F., "Progress in the Development of Graphite-Aluminum Composites Using Liquid Infiltration Technology," Journal of Composite Materials, Vol. 10, Oct. 1976, p. 279.

4. Marcus, H.L., Dull, D.L. and Amateau, M.F., "Scanning Auger Analysis of Fracture Surfaces in Graphite-Aluminum Composites," in Failure Modes in Composites IV, J.A. Cornie and F.W. Crossman, eds. Conference Proceedings, The Metallurgical Society of AIME, Fall 1977.

5. Davis, L.E., et al, Handbook of Auger Electron Spectroscopy, Published by Physical Electronics Industries, 2nd edition, 1976.

Table 1

Composite Materials	Processing Technique	*Transverse Strength MPa	Phase(s) Observed in TEM
T114A	Celion 6000, C-100M(s)(s)/6061(Ti+B)	76	TiB_2, Al_2O_3Y
G3842 (made from T133)	VSB-32, C-105-12,(s)/6061(Ti+B)	31	TiB_2, Al_2O_3Y TiC
T105A (plate:G3636)	VSB-32, $\{SiCl_4+BCl_3\}_{730}^{700}$, (s)/6061(Ti+B)	10	TiB_2, Al_2O_3Y TiC
T109B	VSB-32, $\{CH_3SiCl_2+CH_3SiCl_3\}_{480}$ (s)/ 6061(Ti+B)	not available	TiB_2
HM pitch/ 6061	HM 3000 (s), /6061(Ti+B)	14-80 depends on consolidation process	TiB_2

*Transverse Strength was tested in plate forms by Aerospace Corporation.

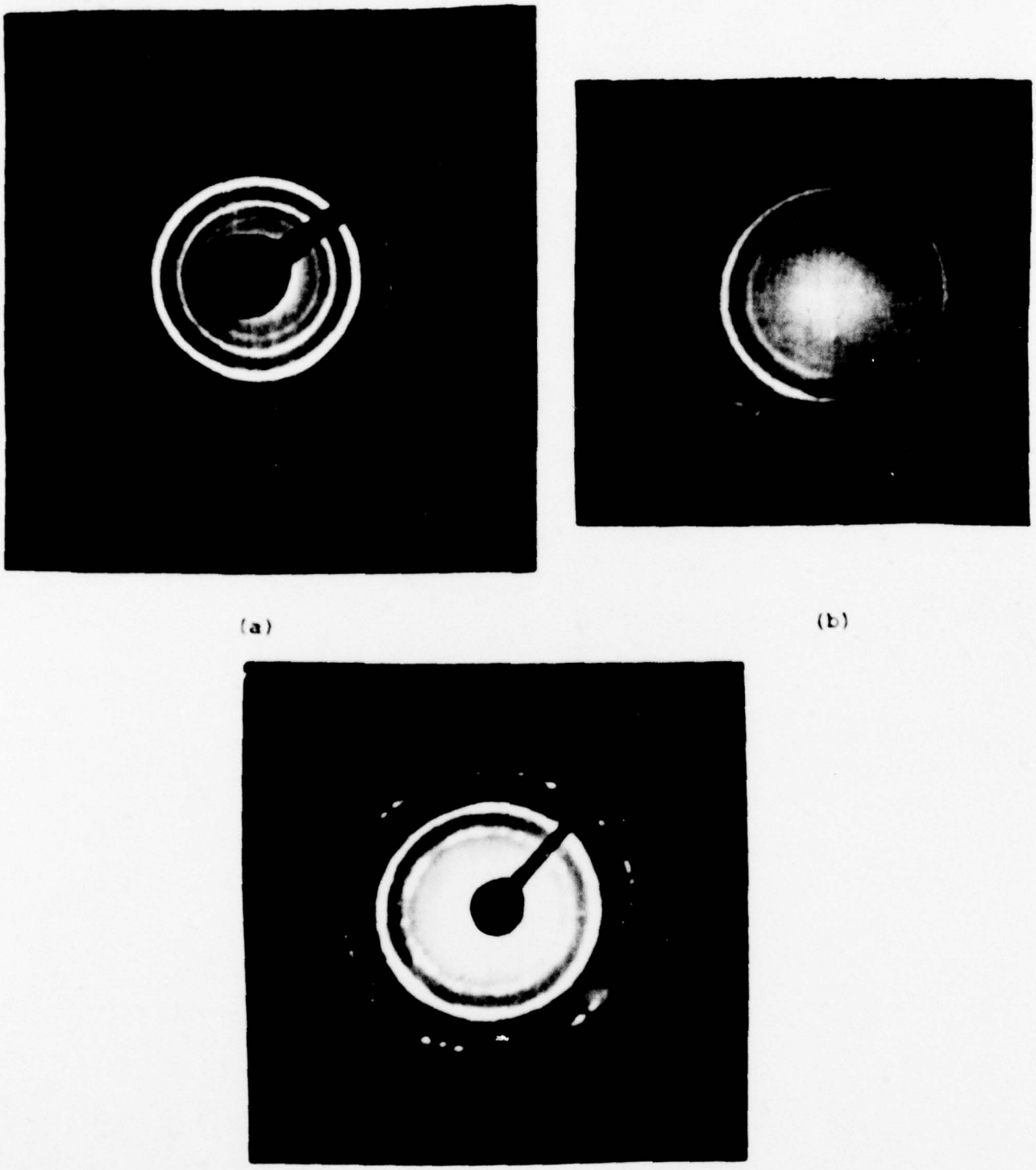

Fig. 1 The electron diffraction patterns for TiB_2 in (a) T105A, (b) G3842, (c) T114 etched by HCl and Methanol.

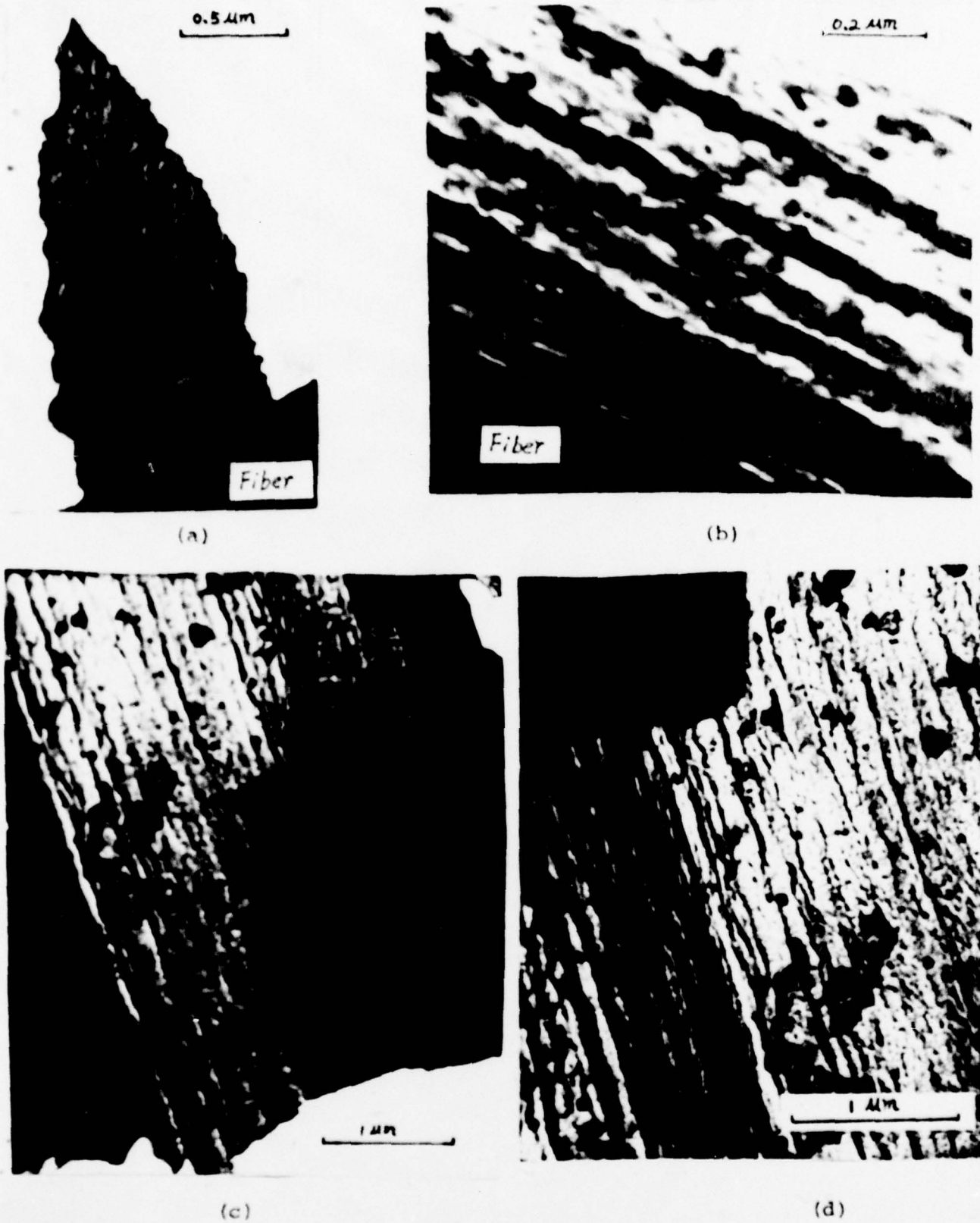

Fig. 2 The electron micrographs showing the crenulated TiB_2 layers in various pitch fiber type composites (a) T109B etched by HCl, (b) T105A, (c) and (d) G3842 etched by HCl and methanol.

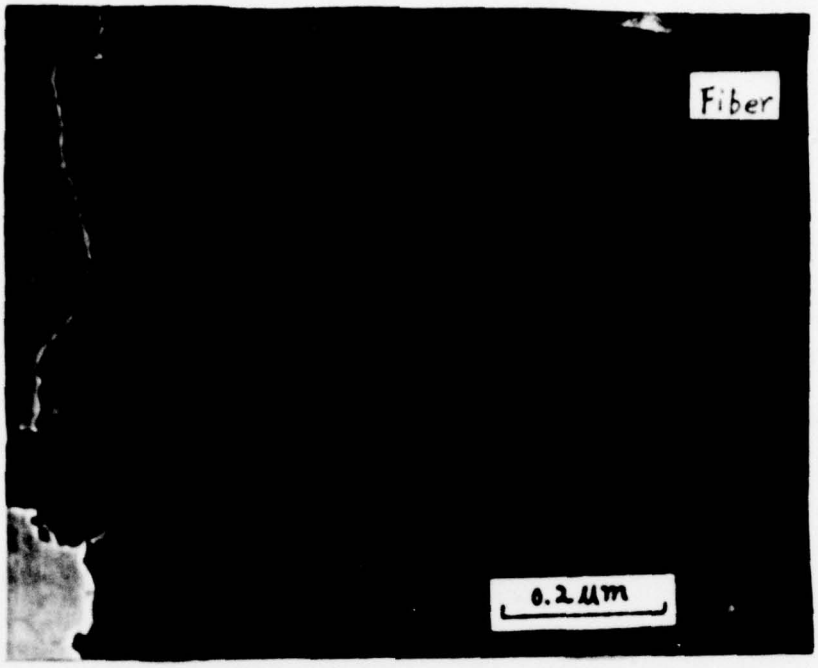

(a)

(b)

Fig. 3 The electron micrographs of larger grain size TiB_2 phase in T114A (a) sample etched by KOH, (b) sample etched by HCl at higher magnification.

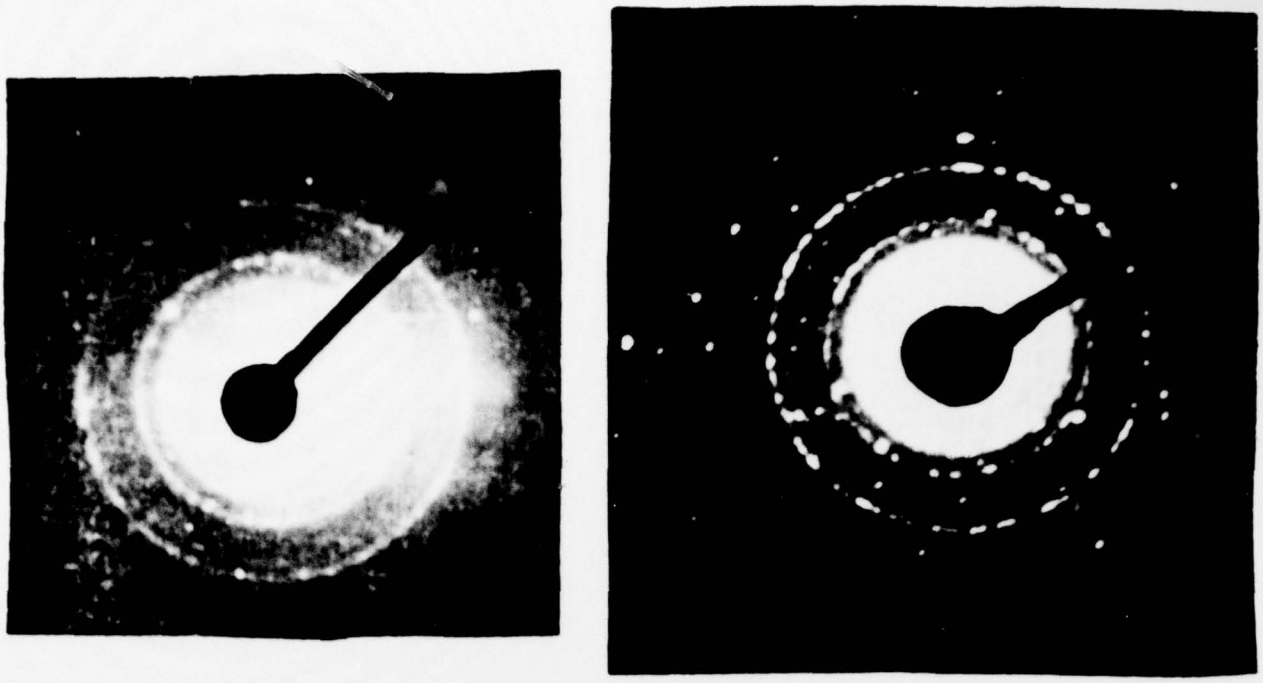

(a)

(b)

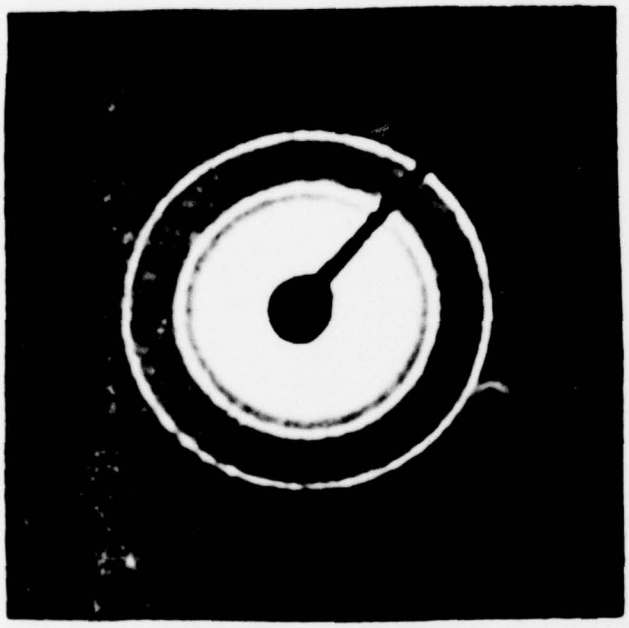

(c)

(d)

Fig. 4 Electron diffraction patterns of $Al_2O_3\gamma$ phase in (a) and (b) T114A etched by HCl, (c) G3842, (d) T105A etched by HCl and methanol. In (d) TiB_2 phase also appeared. All oxides showed larger grain size.

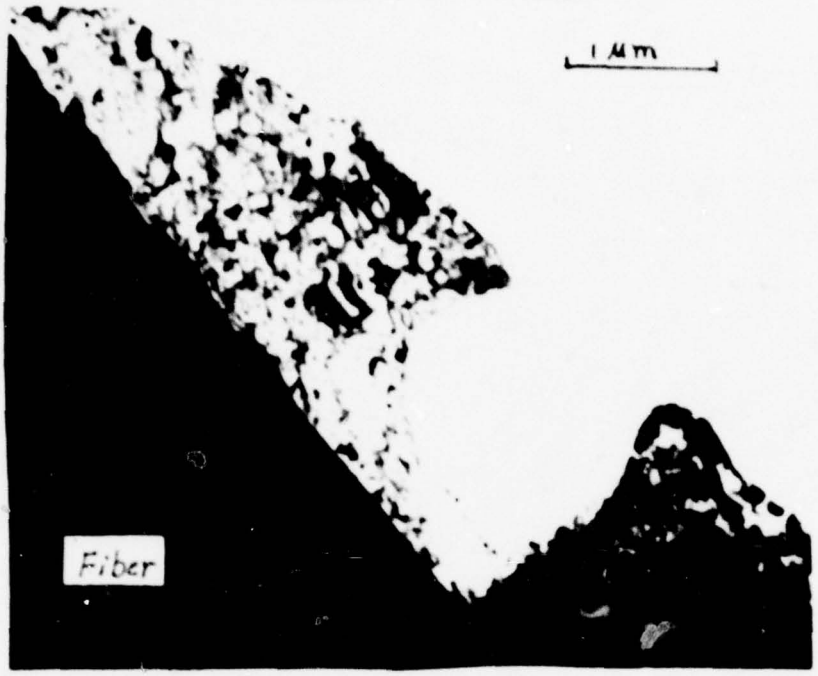

(a)

(b)

Fig. 5 The micrographs showing $Al_2O_{3\gamma}$ phase in T114A etched by HCl and methanol. (a) Low magnification of whole piece, the dark part is graphite fiber, (b) High magnification of center area of the lighter part in (a). Note: some larger grain TiB_2 was also found in the narrow neck part of the whole piece in (a).

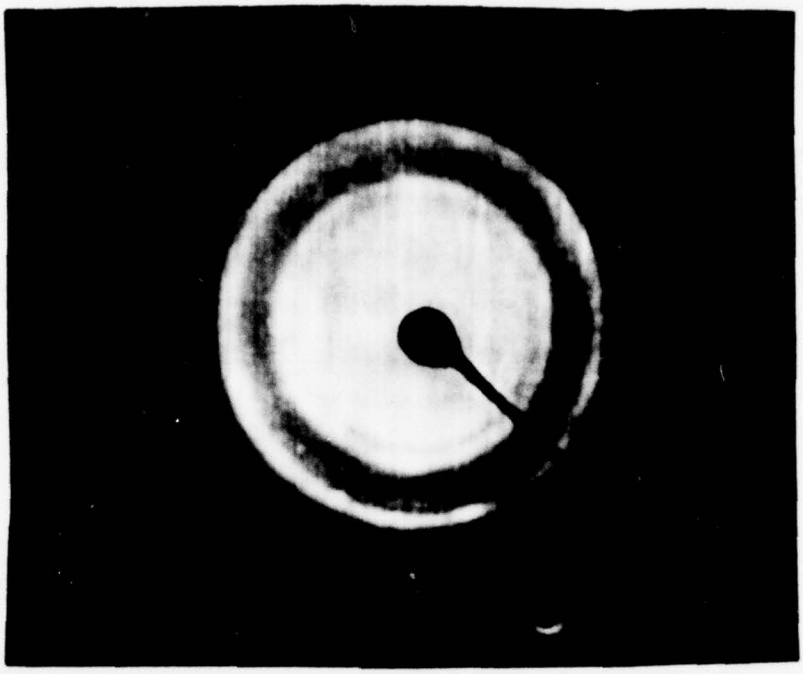

(a)

(b)

Fig. 6 The TiC phase in G3842 etched by KOH (a) a diffused electron diffraction pattern, (b) the micrograph of (a).

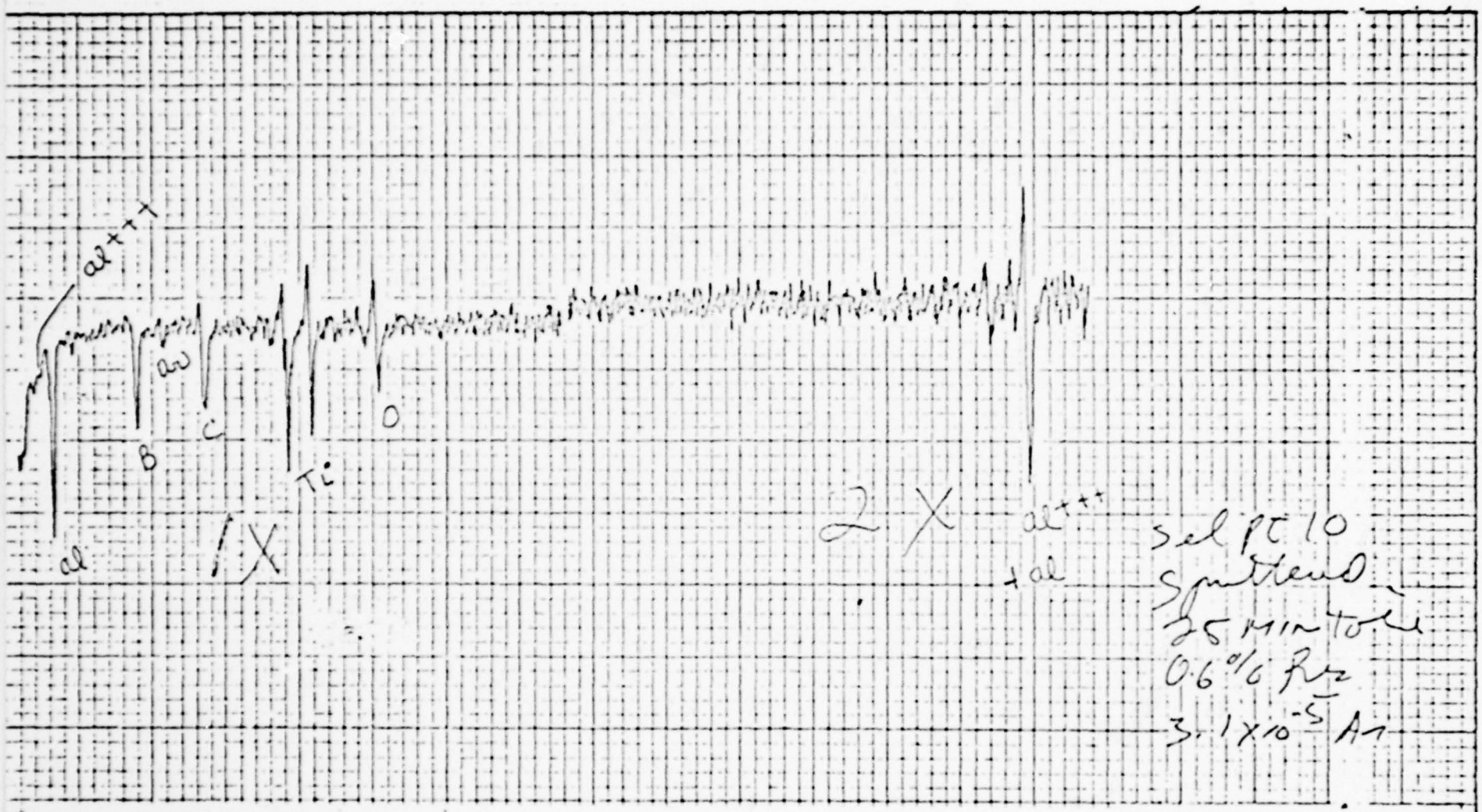

Fig. 7 AES analysis of the fractured interface after 25 minute sputtering in T105A (plate G3636 was used).

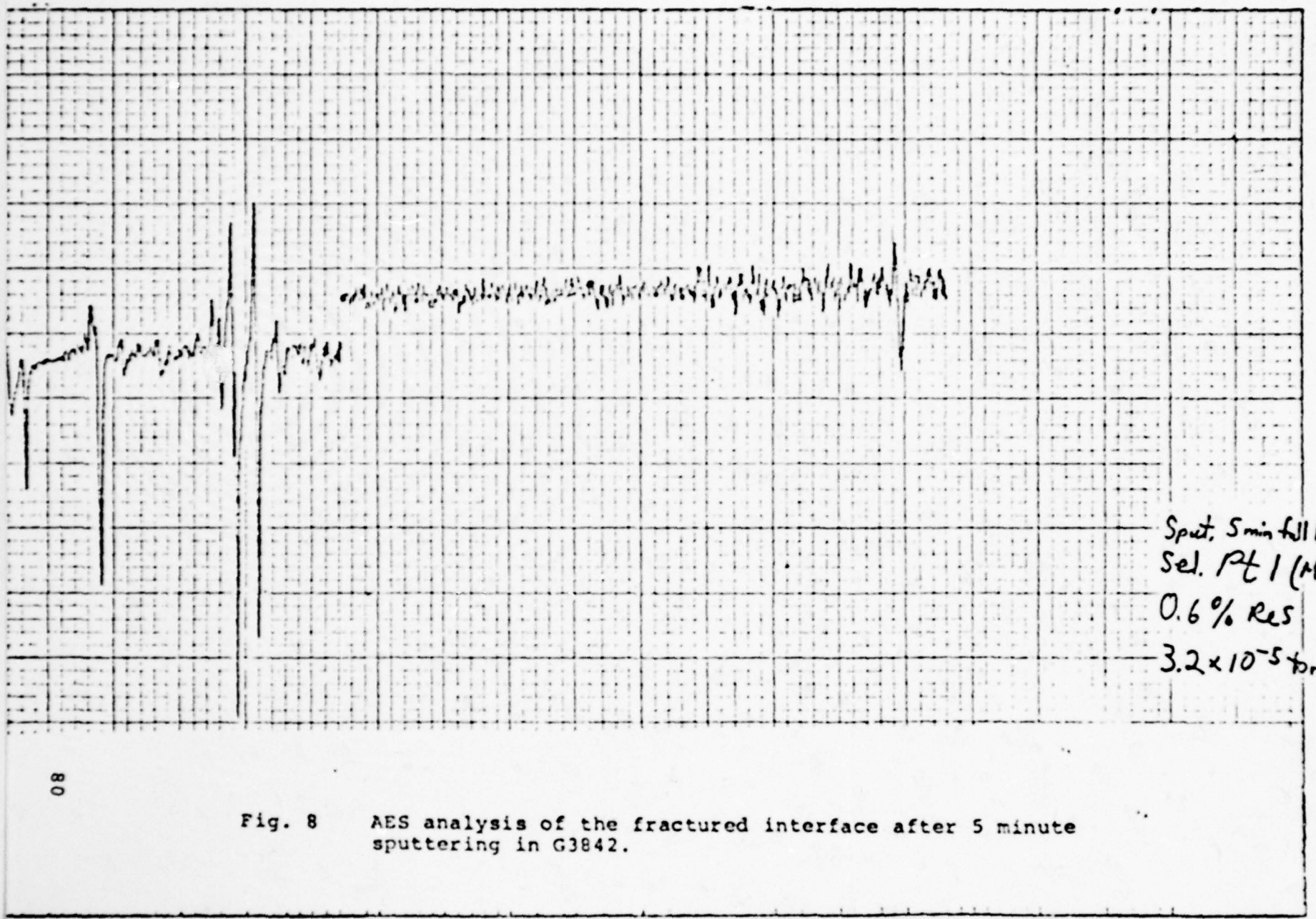

Fig. 8 AES analysis of the fractured interface after 5 minute sputtering in G3842.

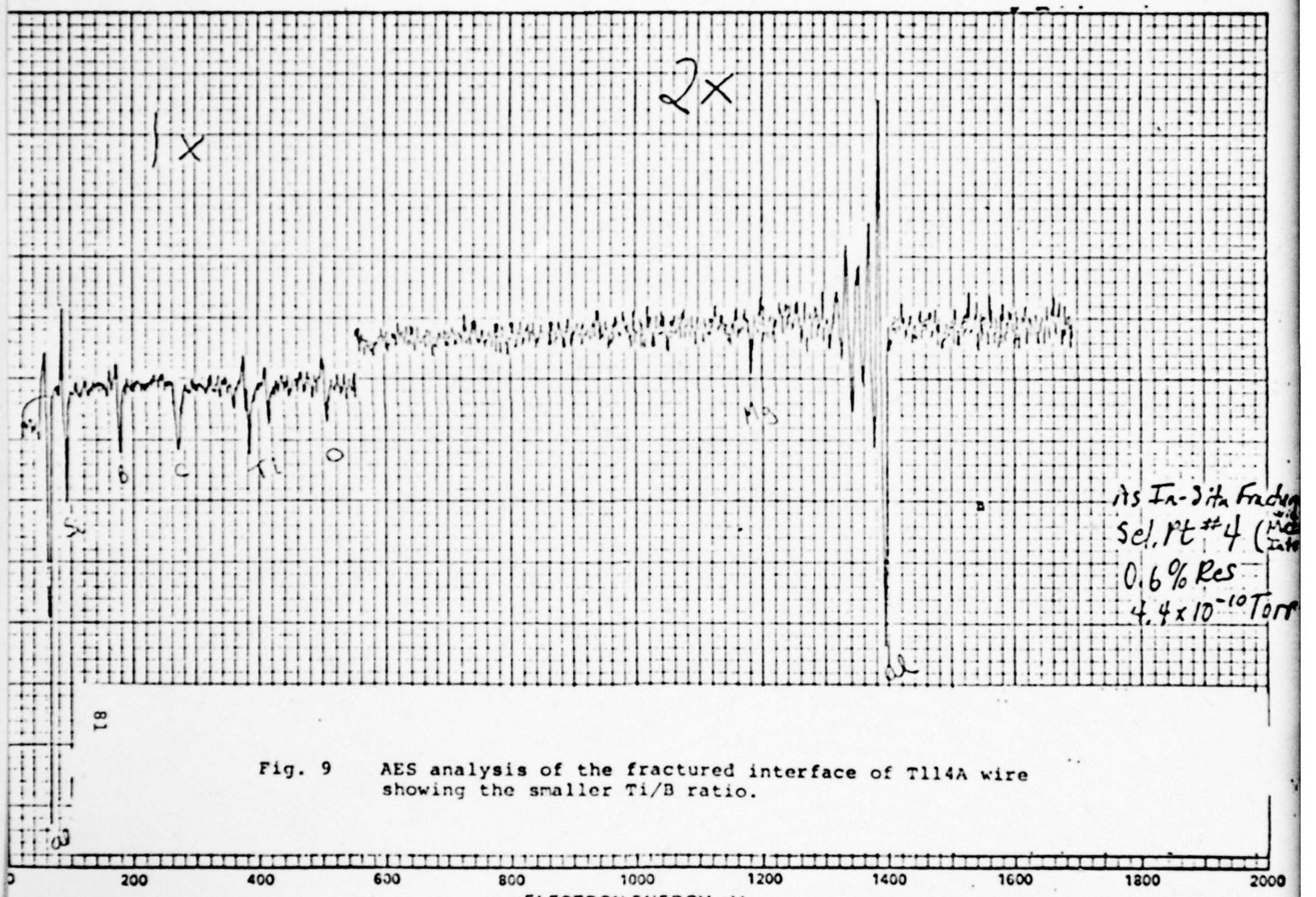

Fig. 9 AES analysis of the fractured interface of T114A wire showing the smaller Ti/B ratio.

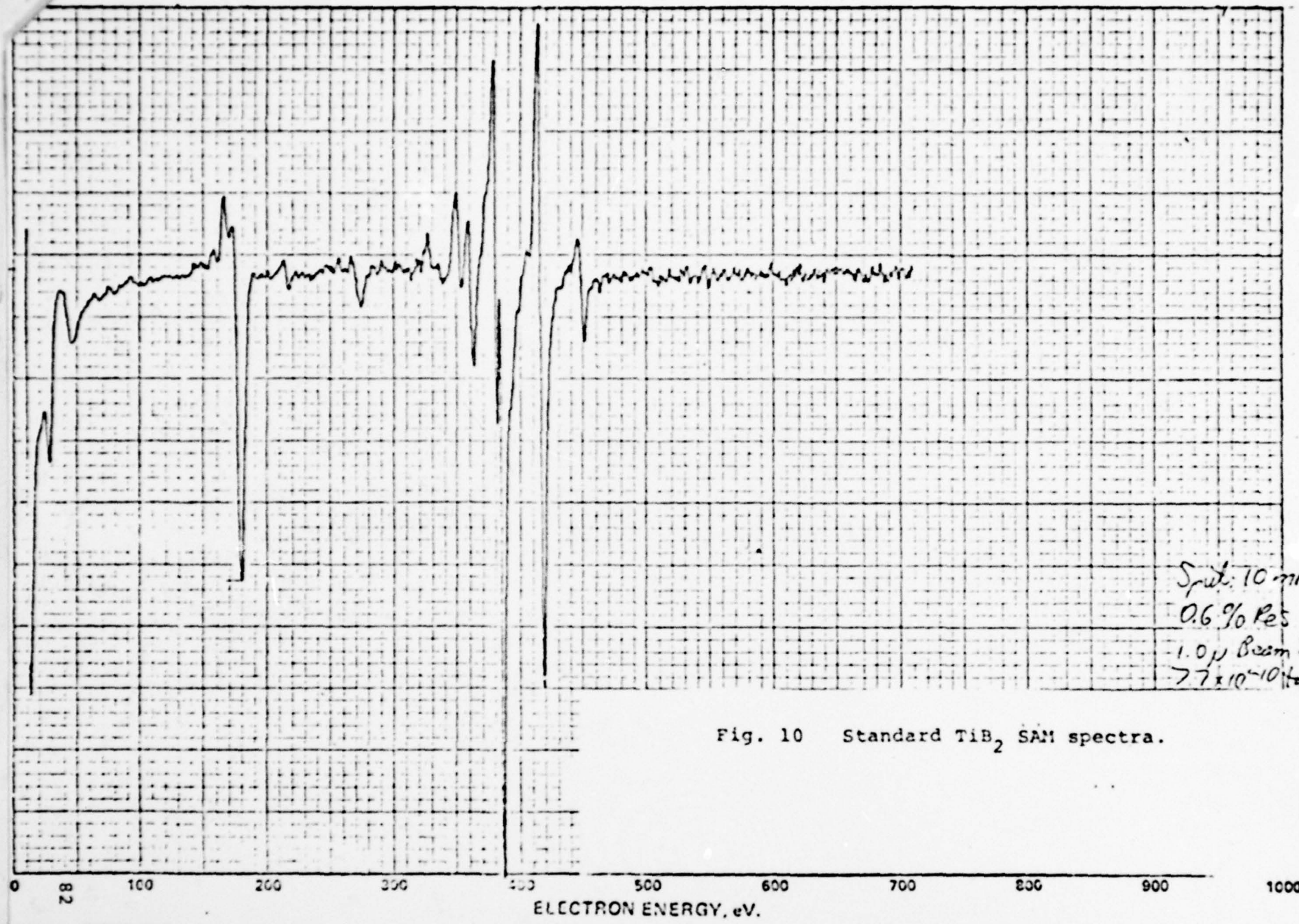

Fig. 10 Standard TiB_2 SAM spectra.